ADVANCED MATERIALS
www.advmat.de

Tailoring Interfacial Structures to Regulate Carrier Transport in Solid-State Batteries

Zhikang Deng, Shiming Chen, Kai Yang, Yongli Song,* Shida Xue, Xiangming Yao, Luyi Yang,* and Feng Pan**

Solid-state lithium-ion batteries (SSLIBs) have been considered as the priority candidate for next-generation energy storage system, due to their advantages in safety and energy density compare with conventional liquid electrolyte systems. However, the introduction of numerous solid-solid interfaces results in a series of issues, hindering the further development of SSLIBs. Therefore, a thorough understanding on the interfacial issues is essential to promote the practical applications for SSLIBs. In this review, the interface issues are discussed from the perspective of transportation mechanism of electrons and lithium ions, including internal interfaces within cathode/anode composites and solid electrolytes (SEs), as well as the apparent electrode/SEs interfaces. The corresponding interface modification strategies, such as passivation layer design, conductive binders, and thermal sintering methods, are comprehensively summarized. Through establishing the correlation between carrier transport network and corresponding battery electrochemical performance, the design principles for achieving a selective carrier transport network are systematically elucidated. Additionally, the future challenges are speculated and research directions in tailoring interfacial structure for SSLIBs. By providing the insightful review and outlook on interfacial charge transfer, the industrialization of SSLIBs are aimed to promoted.

1. Introduction

The present conventional lithium ion batteries (LIBs) with liquid electrolytes have been widely used for portable electronics.[1–3] However, potential safety issues hinder their practical application in electric vehicles due to the flammability and volatility of organic liquid electrolyte.[4–7] Besides, the fast-growing markets of EVs and grid-scale energy storage devices require high-energy density batteries, as well as excellent safety.[8] Therefore, solid-state lithium ion batteries (SSLIBs) have emerged and become the most promising candidates for next-generation energy storage system.[9–12] SSLIBs equipped with non-flammable and stable solid electrolytes (SEs) have circumvented the most safety issues in LIBs. For instance, organic liquid electrolytes are prone to evaporate at temperatures higher than 60 °C, leading to the expansion of pouch cell and irreversible degradation of batteries.[13] By contrast, SEs exhibit the high thermal stability (300~800 °C), which avoids the occurrence of thermal runaway.[14] Furthermore, SEs show a relatively wider electrochemically window compared with that of liquid electrolytes which facilitates the application of electrodes with much higher energy density.[15] Extensive efforts have been made to design and synthesize SEs, including inorganic solid electrolytes (ISEs) and organic-based polymer solid electrolytes (SPEs). Compared with SPEs, ISEs—such as LISICON-type, NASICON-type, perovskite-type, garnet-type, halide-type and sulfide-type, exhibit higher ionic conductivities of $\approx 10^{-2}$ S cm^{-1} at room temperature. However, they also suffer from more serious interface issues, which are the primary focus of this review.

In fact, liquid electrolytes could permeate into the whole electrodes and separator readily, establishing effective and percolative ion transport network among cathode and anode. However, these beneficial liquid-solid interfaces become solid-solid interfaces when the liquid electrolyte and porous separator are replaced by SEs. Rigid and insufficient contact between active materials and SEs will hinder the Li^+ diffusion and decrease the rate capacity, which will be aggravated if the cracks formed owing to the localized stress during electrochemical cycling.[16] Undesirable electron (e^-) transfer at the electrode/SE interface will trigger chemical side reaction and the resulting formation of the inactive decomposition interlayers, leading to high interfacial resistance and even structural collapse of cathodes.[17,18] Moreover, the localized current density gradient on the grains and the

Z. Deng, S. Chen, S. Xue, X. Yao, L. Yang, F. Pan
School of Advanced Materials
Peking University
Shenzhen Graduate School
Shenzhen 518055, China
E-mail: yangly@pkusz.edu.cn; panfeng@pkusz.edu.cn
K. Yang
Advanced Technology Institute
Department of Electrical and Electronic Engineering
University of Surrey
Guildford, Surrey GU2 7XH, UK
E-mail: kai.yang@surrey.ac.uk
Y. Song
School of Energy and Power Engineering
Jiangsu University
Zhenjiang 212013, China
E-mail: songyl@ujs.edu.cn
The ORCID identification number(s) for the author(s) of this article can be found under https://doi.org/10.1002/adma.202407923

DOI: 10.1002/adma.202407923

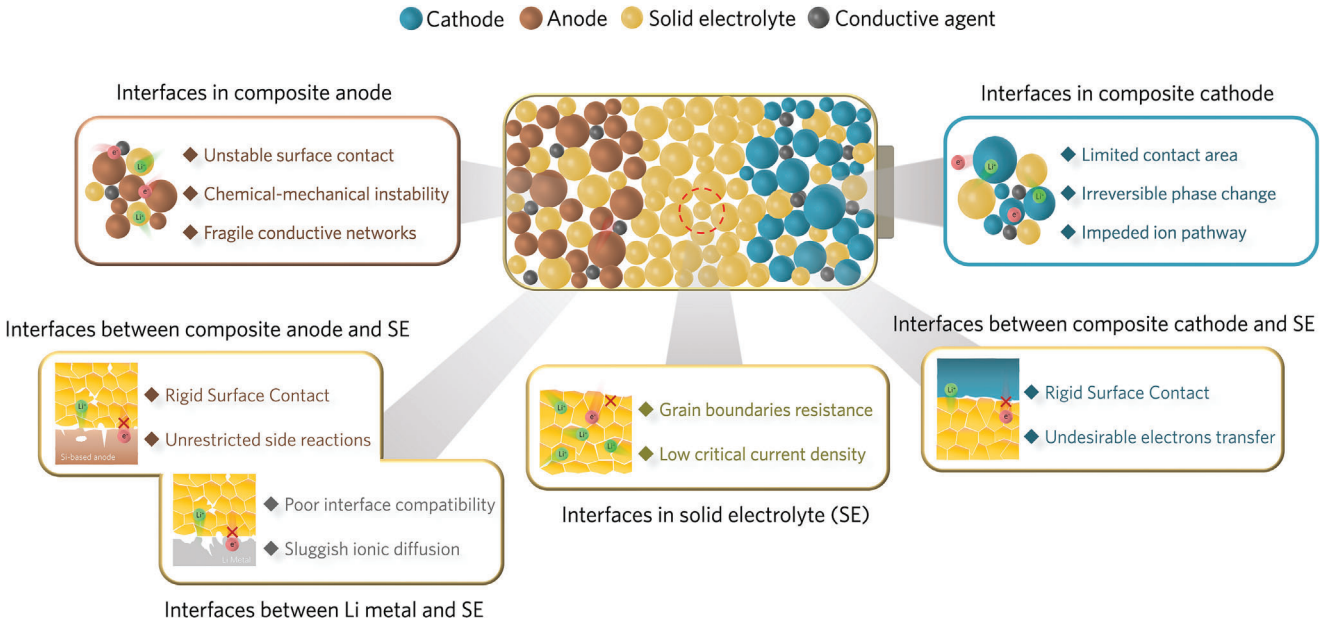

Figure 1. Schematic illustration of various interface issues in SSLIBs.

interface of Li metal and SEs may trigger lithium dendrite growth and internal short-circuit.[19] The extensive commercialization of practical solid-state batteries is impeded by various interfacial problems (summarized in **Figure 1**). Evidently, the interfaces in SSLIBs involve complex charge carriers (i.e., Li^+ and e^-) transport mechanism. Hence, an in-depth understanding on interface evolution process is indispensable on the performance optimization of SSLIBs.

Herein, we categorized the multi-scale interfaces of SSLIBs into internal interfaces (interfaces within composite electrode and SEs) and apparent interfaces (interfaces between composite electrodes and SEs). Based on the issues related to carrier transport at various interfaces, a systematic review of interfacial modification strategies is conducted. The physicochemical processes and interfacial interaction mechanisms during cycling are discussed in detail. Additionally, the optimization strategies and design principles of SSLIBs were further elucidated, aiming to achieve a robust carrier (i.e., Li^+ and e^-) conductive network. Meanwhile, the perspectives on thick electrode design, manufacturing technology and interfacial optimization/characterization are proposed for the future development of SSLIBs, offering fundamental guidance toward commercial applications.

2. Internal Interfaces within SEs

Different from liquid electrolytes, the SEs are mostly inhomogeneous with grain boundaries (GBs) which frequently exhibit undesirable characteristics such as low ionic conductivity, high electronic conductivity, and poor mechanical strength. The presence of voids and gaps among the grains generates an extra obstacle for the transport of Li^+, resulting in the reduced ionic conductivity and the agminated Li^+ at these boundaries.[20] Moreover, the GBs of some SEs (e.g., $Li_7La_3Zr_2O_{12}$ (LLZO)), exhibit a high level of electron conductivity, enabling e^- along the boundaries to couple with Li^+, leading to the reduction of Li^+ ions to Li^0, strongly perturbing the electronic structure and causing the growth and spread of lithium dendrites along the GBs.[21] Therefore, constructing a rapid ionic conductive network while suppressing e^- conduction in SE is highly desirable.

2.1. Li^+ Diffusion on Grain Boundaries

The ionic bulk conductivity for some of the SEs is sufficiently high for actual application ($Li_{3x}La_{2/3-x}TiO_3$ (LLTO), $Li_{1+x}Al_xGe_{2-x}(PO_4)_3$ (LAGP), $Li_{1+x}Al_xTi_{2-x}(PO_4)_3$ (LATP)),[22,23] however the total ionic conductivity is actually orders of magnitude lower due to the poor GBs conductivity. GB is present when two particles with different orientation in polycrystalline samples contact. In addition, space-charge layers are usually formed at the GBs under two scenarios:[24] (1) the different conduction properties of Li^+ and the potential barrier effect of the GBs, which results in Li^+ accumulating close to the GBs; (2) the different conduction properties of e^- at the GBs, causing e^- accumulation (**Figure 2A**). The space-charge layer might greatly suppress the ionic conductivity at the interface and result in a high migration energy barrier (Figure 2B) in these areas.[25,26] For instance, in LLZO-based SEs, GBs contributions to the total resistance are close to 50% at different temperatures.[27] For LLTO, it was found that most GBs comprised severe structural and chemical deviations at atomic-scale, especially the depletion and restriction the transport of the charge carrier Li^+ greatly increased the GBs resistance.[22,28] While in NASICON-type LAGP and LATP, the origin of the GBs resistance is generally caused by the irregular arrangement of GBs atoms and the generation of insulating impurity phases.[29–31] However, it is sometimes difficult to achieve both high relative density and GBs ionic conductivity in LATP due to the insufficient sintering conditions, ultra-high temperature (above 1000 °C) and suboptimal grain (non-optimal grain size and impurities at the GBs).[32]

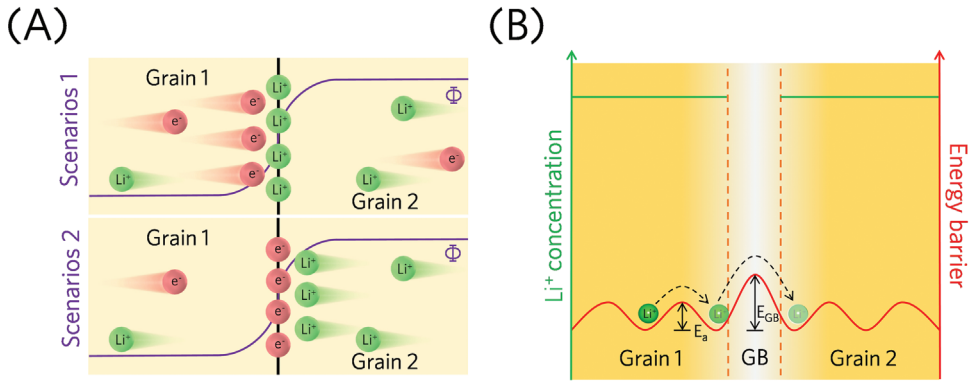

Figure 2. A) Two scenarios of the space-charge layer forms at the GBs, Φ represents Galvani Potential. B) Energy barrier and variation in Li^+ concentration throughout the GB. The activation energies in grains and GBs are denoted as E_a and E_{GB}, respectively.

Different strategies have been developed to increase the ionic conductivity in GBs by improving bulk microscopic anisotropic properties such as grain size, shape, orientation, and porosity distribution of the SEs as such. (1) Controlling the size and orientation of the grains can influence the roughness at the interface and the microscopic characteristics (e.g., stress distribution) throughout the bulk (**Figure 3A**).[33] In that case, a heating densification technique (1100 ~ 1300 °C) and e^- backscatter diffraction were adopted to control the grain size of LLZO while obtaining optimal grain size and orientation. The increased grain size reduced the GBs area and hence the number of probable failure points, thereby improving the consistency of SEs.[34] (2) Li^+ transport across the GBs usually forms a space-charge layer, which results in a high migration energy barrier in these areas. Reconstruction of the GBs interface with high-conductive amorphous domains can solve this problem. The amorphous layer creates extra vacant sites for Li^+, preventing the accumulation of Li^+ at the GBs, effectively reducing the potential barrier, and finally significantly enhancing the ionic conductivity.[35,36] (3) The anisotropy of grains creates a potential barrier that hinders the movement of Li^+ through grains, and this barrier cannot be altered by high-temperature sintering.[37] Therefore, some isotropic glass additions like lithium boron oxide with good wetting properties can be introduced to coat the pores and fill the grain, facilitating the movement of Li^+ along the electrolyte grains and over the SEs/electrode while minimizing the conduction barrier.[38,39] (4) Developing efficient sintering strategies to prepare SEs with dense microstructures and excellent conductivity. For example, sintering with hot pressing can improve grain-to-grain adhesion and minimize GBs impedance.[40] Besides, the addition of sintering agents such as Al_2O_3, which can eliminate Li_2CO_3 at GBs by promoting the decomposition, enhance the sintering process, and establish a rapid Li^+ conducting network along the GBs with the concomitant product $LiAlO_2$, results in a substantial increase in the ionic conductivity of SEs (Figure 3B).[41] Other special synthesis techniques, like spark plasma sintering, use this technology to create high-density SEs with excellent electrochemical performance (ionic conductivity, electrochemical stability) at relatively low synthesize temperatures and short processing times.[42] (5) Except for sintering techniques, the coprecipitation method[43] and sol-gel process[44] could also be effective strategies to prepare LATP. Through precursor selection and optimization of synthetic routes, GB and impurity formation can be reduced.

2.2. Electron Diffusion on Grain Boundaries

Previous results have already indicated that garnet SEs (e.g., LLZO) usually have a low critical current density (CCD)[45,46] and high electrical conductivity.[47] CCD can be defined as the highest current density when SSLIBs go through internal short-circuit and the propagation of the lithium dendrites within the SEs.[48] In contrary to the intuitive concept that mechanically hard SEs could suppress the lithium dendrites, short circuit occur in SSLIBs under even lower current densities than liquid electrolyte-based batteries.[49] Ideal SEs are expected to possess high ionic conductivity and low electrical conductivity, however, recent studies have shown that the low CCD is highly correlated to the high electronic conductivity at the GBs, where Li^+ are reduced by e^- to form metallic Li.[20] In addition, first-principles investigation was also adopted to find the reason for the high electronic conductivity at the LLZO GBs. It reveals that the excess e^- show strong affinity to be localized in ZrO_5 units at the GBs. When apply an exterior voltage, the extra e^- tend to become delocalized, leading to a higher electronic conductivity at the GB.[50] Furthermore, it has been widely assumed that the short-circuiting mechanism in garnet SEs is similar to that in liquid electrolytes, where Li dendrites first nucleate at the Li/electrolyte interface and propagate along GBs or through voids between ceramic particles. Our previous work proposed a model to reveal the short-circuit mechanism of $Li_7La_{2.75}Ca_{0.25}Zr_{1.75}Nb_{0.25}O_{12}$ (LLCZN), found that e^- transfer more easily within the SEs when external electric field exceeds threshold voltage, which will promote the reduction of the Li^+ and the formation of Li^0 at the GBs as the origin of the internal short-circuit (**Figure 4A**).[51]

To lower the electronic conductivity at GBs and increase the CCD of SEs, several approaches have been devised. (1) A grain-boundary electronic insulation strategy is proposed, where electronic insulation materials that possess extremely low electronic conductivity and high humidity stability are introduced in GBs modifications. Poly (ethylene glycol) dimethyl ether (PEGDME) is chosen as one decoration material to modify the GBs of Li_6PSCl_5 (LPSCl), which can increase the e^- transfer

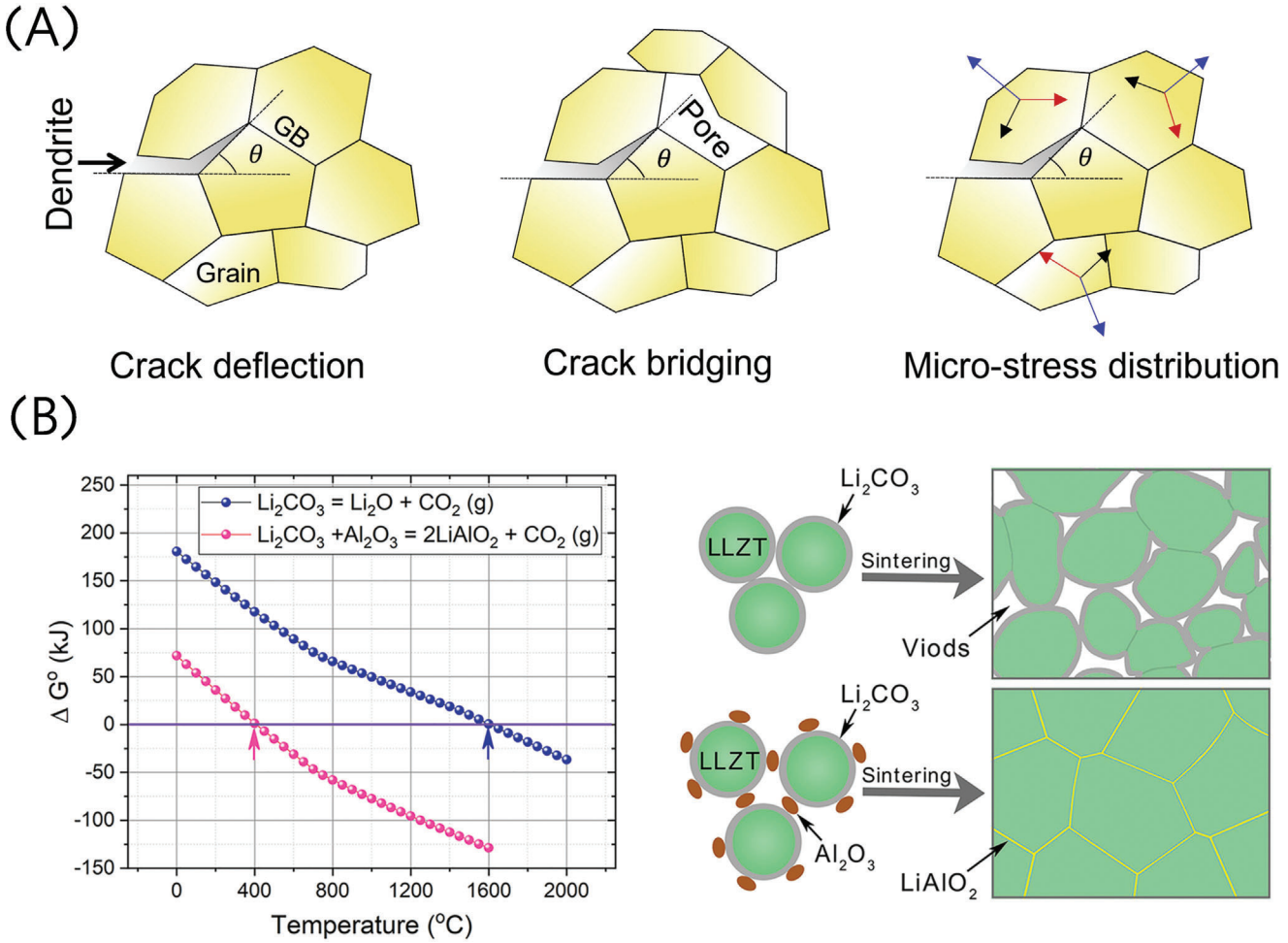

Figure 3. A) Schematic of the microscopic characteristics (crack deflection, crack bridging, and elastic anisotropy due to varying grain orientation) throughout the bulk. Reproduced with permission.[33] Copyright 2020, Elsevier. B) Gibbs free-energy versus temperature curve for decomposition of Li_2CO_3 with and without Al_2O_3; Illustration of function of Al_2O_3 additive in sintering process of $Li_{6.5}La_3Zr_{1.5}Ta_{0.5}O_{12}$ (LLZTO).[41]

energy barrier so that block e^- transport across the LPSCl GBs (Figure 4B).[52] (2) Surface engineering on the surface of SEs such as the introduction of $LiAlO_2$ (Figure 4C),[53] LiF[54] and Li_3P[55] with interstitial filling capability and low electronic conductivity, will result in improved insulation properties of SEs and CCD values. (3) The use of laser annealing and the resulting formation of amorphous interface with wide bandgap to prevent the entry of e^- into the GBs (Figure 4D),[56] have been proven to decrease the e^- transfer. (4) Applying appropriate pressure through a constant pressure cell architecture can effectively inhibit the increase in local current density by reducing the voids (Figure 4E).[57] Besides, the mechanical constriction technique applied to $Li_{10}GeP_2S_{12}$ (LGPS) can not only increase the CCD and inhibit the growth of lithium dendrites, but also prevent the interface electrochemical reaction.[58]

3. Internal Interfaces within Electrodes

The composite electrodes of SSLIBs are generally composed of active materials, electronic conductive agents and SEs. The poor physical contact of solid particles leads to the large carrier transfer impedance which will be aggravated if the cracks formed owing to the localized stress during electrochemical cycling. Besides, Li^+ is transported in a network of active materials and SEs while e^- is transported in a network of active materials and conductive agents. The gap between electronic transport network and ionic transport network hinders the cooperative transport of carriers. It should be noted that chemical and electrochemical stability of interface are discussed in detail in the next section. Hence, the internal interfaces in the composite electrodes need to be regulated rationally to create a percolative carrier transport network among these particles.

3.1. Internal Interfaces within Cathode

The coexistence of cathode active materials (CAMs), electronic conductive carbon and SEs in the composite cathode forms tremendous solid-solid interfaces (i.e., CAMs/SEs interfaces, CAMs/carbon interfaces and SEs/carbon interfaces), leading to the large charge transfer impedance (**Figure 5A**). Besides, the large local strain at the interfaces between CAMs and SEs could

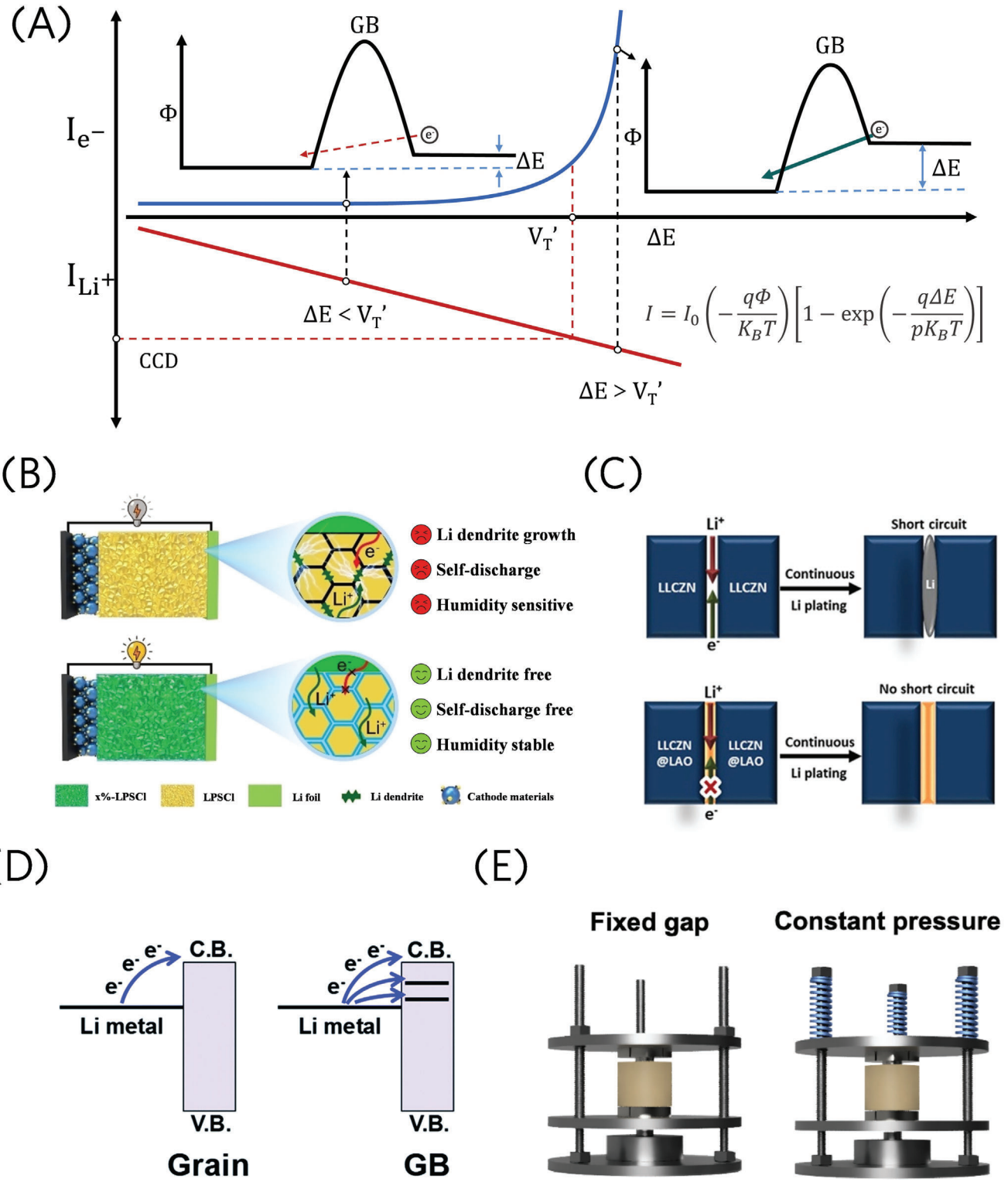

Figure 4. A) Schematic of e^- conduction at GBs with varying external electric field.[51] B) Schematic illustration of ASSLBs using LPSCl and x-LPSCl as electrolytes and their different performance on Li dendrite suppression, self-discharge suppression and humidity resistance.[52] C) Schematic illustration of Li formation within LLCZN and how to suppress it through surface coating.[53] D) Energy band diagrams of grain and GBs of LLZTO. Reproduced with permission.[56] Copyright 2020, Royal Society of Chemistry. E) Schematic of the cell cycling setups for fixed gap and constant pressure. Reproduced with permission.[57] Copyright 2023, Elsevier.

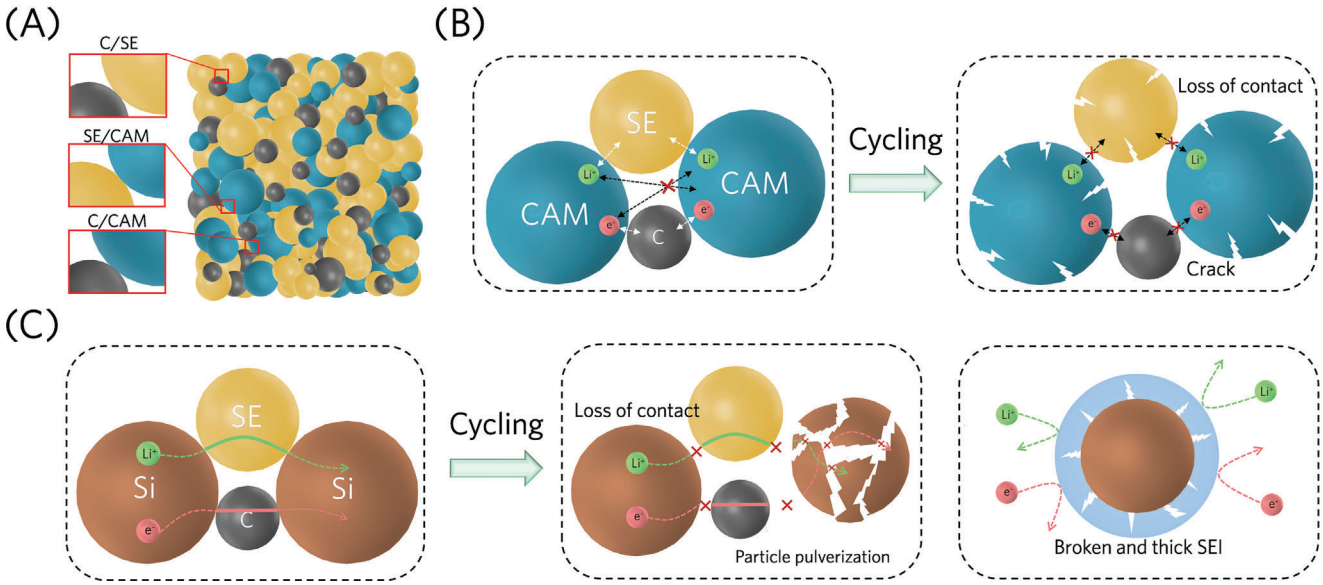

Figure 5. A) Schematic illustration of composite cathode microstructure. B) Schematic illustration of composite cathode failure mechanism. C) Schematic illustration of composite Si anode failure mechanism.

lead to mechanical failures such as crack formation and delamination due to the phase transformation during the cycling (Figure 5B). Besides, the problem will be exacerbated in the high areal capacity (>5 mAh cm^{-2}) cathodes, which suffer the large contact impedance caused by the point contact between particles. Hence, it is essential to achieve the intimate physical contact and sufficient contact area between CAMs and carrier conductors (e.g., SEs and conductive carbon). In addition, it is also necessary to ensure the (electro)chemical stability among the CAMs, SEs and electronic conductive carbon; otherwise, undesired side reactions may occur in the cathode.

3.2. Internal Interfaces within Anode

The dramatically rising price of Li mineral and serious security issues of Li-metal anode impede the development of SSLIBs. Except for Li anode, Si-based anode materials hold the advantages of the ultra-high theoretical specific capacity (1000–4200 mAh g^{-1}), abundant resources (the second largest in the earth's crust) and environmental benignity which are considered as promising anodes for the next-generation SSLIBs. However, significant stresses are generated during the lithiation/delithiation process due to the large volume swing (100~300%), leading to pulverization of the anode particles (referred as mechanical pulverization) and causing the disconnection of electronic/ionic surroundings (referred as conductive environment decay) in anode active materials (AAMs). Simultaneously, the freshly exposed surface of anode particles will surely undergo side reactions with the electrolyte (i.e., sulfide SEs),[59,60] the generation of an unstable and thick solid electrolyte interphase (SEI) layer and ongoing side reaction with SEs promoted by the carbon additives (Figure 5C). In addition, the contact area between AAMs and SEs is constrained within the composite anode, hindering the transportation of e^- and Li^+. Hence, building a robust carrier conducting network in AAMs could be considered as a general strategy to bridge the gap between academic research and practical use.

3.3. Physical Contact of Particles

Because of the random distributions of the irregular particles during homogenate, active material particles (AMPs), SEs and conductive agents formed nonuniform interface pore structures. Such pores or voids space formed during composite electrode preparation will immediately disrupt carrier movement through interface, making the ionic and electronic transport pathway become tortuous. In terms of morphological structure, the ideal composite electrode shape would have minimal void and pore space and sufficient particle contact between SEs and conductive agents. In spite of this, due to the implications of stiffness and surface roughness, atomic-level interaction between irregular heterogeneous particles is practically impossible.

Ensuring tight physical contact between AMPs and SE particles is key to achieving effective ion transport and high electrode utilization. The rigid physical feature of SEs lead to unstable point-contact with AMPs which will continue to produce numerous voids.[61] The point-contact between SEs and AMPs will lead to sluggish ion transport in the interface regions to increase the interfacial resistance and hinder the rate performances.[62] During cycling, the structures contraction and expansion of particles might cause more undesirable voids. Gradually, when the voids congregate to a certain amount, the "dead" area will be created, which is lack of percolation paths so that prevent the transportation of e^- and Li^+.[63] In addition, the charge heterogeneity within the electrode materials and the resulting volume change of the electrode particles would furthermore introduce non-homogeneous distribution of stress and the formation of the cracks (**Figure 6A**),[16,64] which would make the contact loss between particles more severe, destruct the ion diffusion path, and

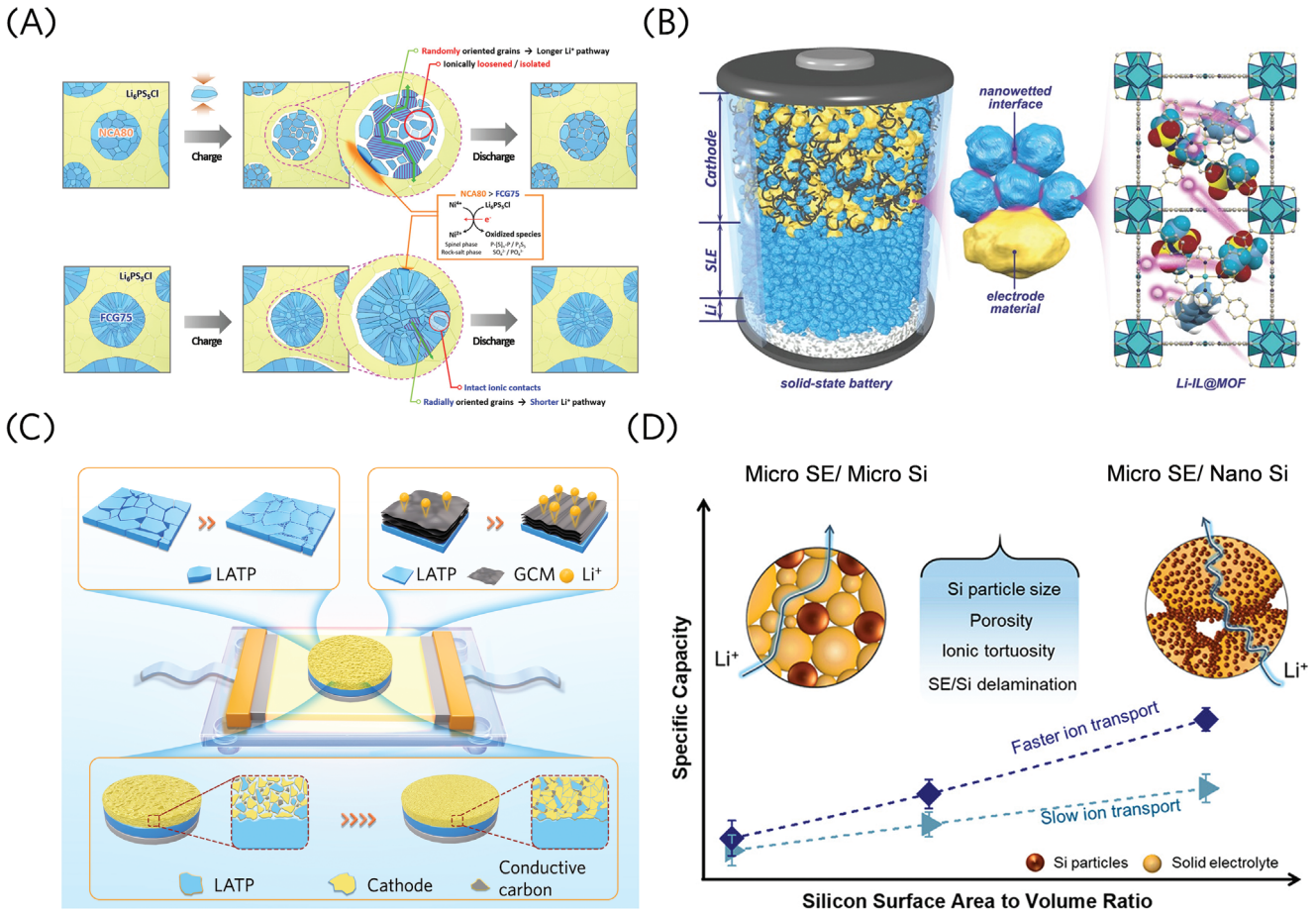

Figure 6. A) Mitigating CAM particle cracking by the use of tailored "full concentration gradient" (FCG) CAM particles with rod-shaped crystallites.[64] B) Schematic illustration for the architecture and nano-wetted interfacial mechanism.[77] C) Schematic illustration of TPS and its impact on CAM/SE contact.[81] D) Influence of Si particle size and ionic conductivity of the SE on the rate performance of the anode composites. Reproduced with permission.[82] Copyright 2023, American Chemical Society.

greatly increase the interfacial resistance. Finally, the formation of the spinel and rock-salt interface during cycling would consume extra Li^+ and decrease the columbic efficiency and cause capacity decay.[65]

Different strategies have been developed to introduce dense contact and hence facilitate the ionic diffusion on the SEs/AMPs interface: (1) Introduction of "void filling" media, such as liquid electrolyte,[66] flexible ion-conducting LiF/graphene interlayer[67] and lithiated Nb_2O_5 diffusion barrier to facilitate interfacial contact between SEs and the AMPs,[68] etc. Besides, in situ coating layer with high-voltage stability while being ionically and electronically conductive on both SEs and AMPs.[69] Such layers serve to shield the electrolyte from oxidation while allowing fast Li^+ transport. (2) Increasing the contact interface by electrode architecture design, such as the synthesis of thin film cathode and solid electrolyte composite electrodes with planar contact[70] and 3D lithium conductive frameworks,[71–74] these structures will facilitate direct atomic-level contact between the AMPs and enable the formation of nano-wetted interfaces, hence promoting the kinetics of Li^+ transport (Figure 6B).[75–77] (3) Operating the SSLIBs under appropriate pressure which can enhance the contact between different components then accommodate the reversible volume change of the electrode, therefore mitigating the influence of the volume effect on the battery performance and inhibiting fractures occurring at the boundary between the SEs and the AMPs.[78,79] (4) Adopting interface welding strategies like hot-press sintering techniques can solve the insufficient contact of particles and effectively lower the CAM/SE interfacial resistance, especially for oxide-based SEs.[80] Besides, our latest research also introduced an effective thermal pulse sintering technique (TPS) that promotes the fusion of the SE and CAM particles interfaces while preventing unwanted phase diffusion (Figure 6C).[81] (5) By reducing the size of AMPs to the nanoscale, the surface-to-volume ratio is increased, resulting in the formation of well-connected conduction routes and sufficient reaction sites at the interface between AMPs and SEs (Figure 6D). This is expected to improve the efficiency of Li^+ transport and promote excellent performance in SSLIBs due to reduced porosity.[82]

3.4. Dispersity of Carrier Conducting Network

To build the composite electrodes, researchers usually add a certain percentage of SEs and electronic conductive additives with

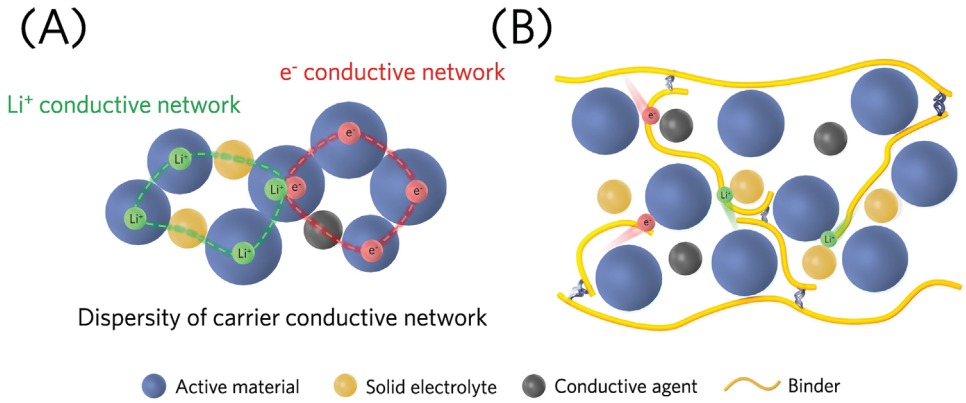

Figure 7. A) The gap between Li^+ conductive network and e^- conductive network. B) Schematic illustration of binders for carrier conducting network in composite electrode.

AMPs to construct the conductive network, where e^- are transferred through limited physical contact between conductive additives and AMPs. The ion conductive network and e^- conductive network are totally different. In that case, the gap between different interfaces lead to the dispersity of networks (**Figure** 7A). Obviously, these conductive networks are both play important role in the efficiency of carrier transportation. Once two networks don't simultaneous response to the exterior voltage, it will cause relaxation phenomenon. In addition, the poor electronic conductivity on the AMPs/SEs interface will result in severe polarization of the interfaces during charging/discharging, which plague the development of SSLIBs.

Improving dispersity requires physical and even chemical homogenization of SEs and conductive additives. The following approaches can be adopted to address these issues: (1) Modifying the surface of AMPs with a carbon coating to increase their electronic conductivity.[83] In addition, carbon nanospheres added to carbon-coated AMPs as a conductivity belt have been proven to play the role of connecting the AMPs, thus creating a short path for Li^+ migration and fast e^- transfer.[84] (2) Introducing ion-electron conducting binders is also one of the strategies (Figure 7B). A specially-designed treating process is presented to create a loosely packed binder with less interconnection force between polymer binder segments and better dispersion performance.[85] Such binders can bridge the gap between the ion conductive network and the e^- conductive network in molecular-level.[86,87] (3) Using nano-structured conductive additives (e.g., carbon nanofibers,[88] multiwalled-carbon-nanotubes[89] and nitrogen-doped carbon nanotube[90]) to achieve better surface contact with AMPs, forming effective percolative carrier-transport pathways among cathode and anode composites and improving reaction kinetics.

To effectively evaluate these improvements, it is crucial to quantify and assess the key metrics of carrier transport networks within composite electrodes, such as ionic tortuosity, ionic/electronic conductivity, and transference number.[91,92] Higher tortuosity indicates more convoluted paths, which can impede ion transport.[93] To measure and calculate these metrics, several methods can be employed. Imaging techniques like scanning electron microscopy (SEM), focused ion beam-scanning electron microscopy (FIB-SEM), and X-ray computed tomography (X-ray CT) provide detailed 3D images for numerical simulations.[94] Electrochemical methods such as electrochemical impedance spectroscopy (EIS) can assess ionic conductivity, while the steady-state current method helps determine the transference number, reflecting the carrier contribution to overall conductivity.[95] Additionally, the four-point probe method could accurately measure the electronic conductivity by eliminating the influence of contact resistance, thus providing precise conductivity values essential for evaluating electronic transport properties.[96] Furthermore, combining advanced imaging with mathematical modeling offers a comprehensive understanding of electrode structures, helping to identify and address transport bottlenecks, thereby improving the performance of SSLIBs.[97]

3.5. Integrity of Carrier Conducting Network

During electrochemical cycling, AMPs will constantly expand and contract in volume because of the lithiation/delithiation process. Among them, Si particles undergo the most significant volume fluctuation, which results in mechanical pulverization and the deterioration of the conductive environment in AAMs. Several approaches have been devised to tackle these problems: (1) Employing straightforward and commercially viable coating techniques, such as carbon coating,[98] polymer coating[99] and metal oxide coating,[100] it is possible to enclose AAMs within those coating layers. The resultant soft layer exhibits the ability to withstand the dynamic interface alterations that occur during volume expansion, hence enhancing the stability of the SEI, preventing its unrestrained growth, and demonstrating exceptional carrier transport capability to optimize the carrier conducting routes. (2) Applying appropriate external pressure, the volume expansion of Si particles could be restricted, and the cracking degree could be reduced by lowering the Von Mises stress, thereby limiting the lithiation process and maintaining the ion-electron contact (**Figure** 8A). This, in turn, inhibits the growth of the volume and prevents the mechanical pulverization of the AAM structure.[101,102] (3) Improving composite electrode preparation technology, such as refining the slurry-mixing technique,[103,104] reducing the size of Si particles,[82,105] adopting two-step wet process and dry process instead of the conventional one-step wet

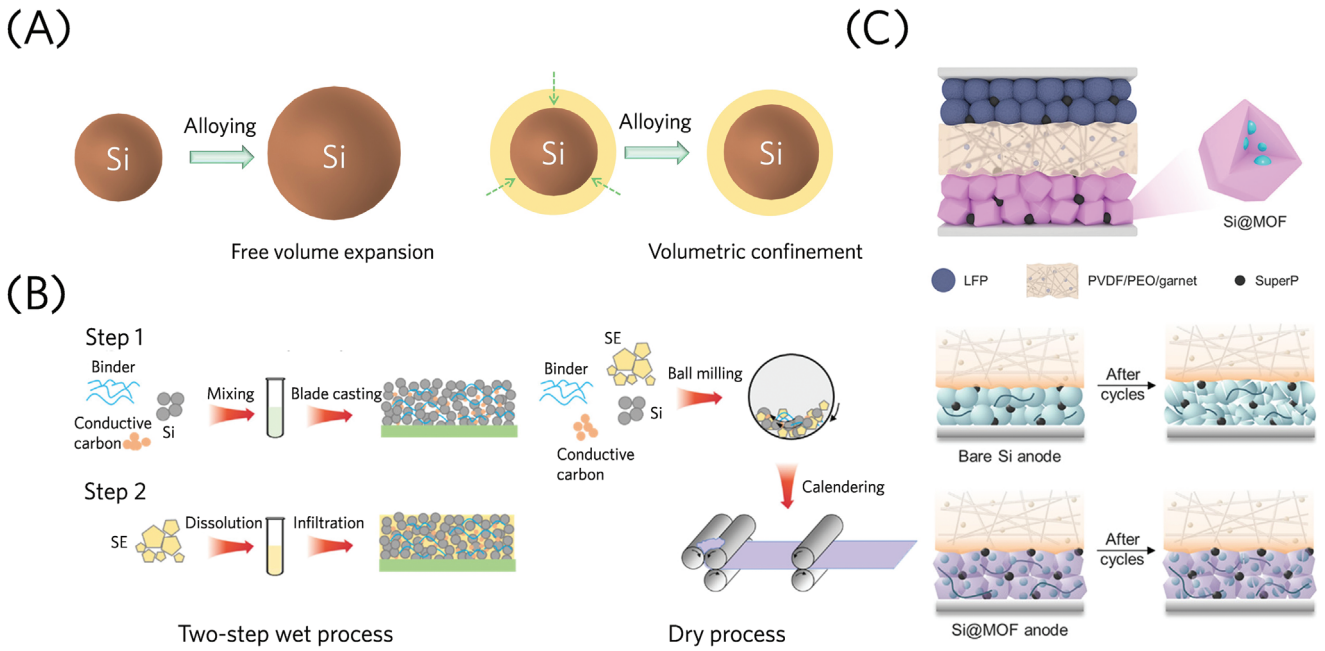

Figure 8. A) Schematic illustration of Si particle under free and external pressure conditions. B) Schematic of the two-step wet and dry process for the preparation silicon composite anodes. Reproduced with permission.[106] Copyright 2022, American Chemical Society. C) Schematic illustration of interfacial evolution for bare Si or the Si@MOF anodes. Reproduced with permission.[107] Copyright 2022, American Chemical Society.

preparation process (Figure 8B).[106] These methods can produce homogeneously dispersed composite electrodes, which leads to a significant enhancement in the contact area. Consequently, Si nanoparticles will show homogeneous distributions in the SEs, resulting in a higher level of consistency. (4) Designing special nanostructures such as metal–organic framework,[107] 3D core-shell nanoparticles,[108,109] porous/hollow Si nanoparticles[110–112] and 1D Si-based nanostructures (Figure 8C).[113] The mechanical strain at the interface, caused by a significant change in volume, can be reduced by the design of nanostructures, resulting in improved stability of the interface and accelerated charge-transfer kinetics. (5) Conventional binders are not suitable for AAMs accompanying large volume expansions.[114] In that case, developing multifunctional binders with high e^- conductivity and mechanical properties can maintain the integrity of conductive networks and the electrode structure.[115,116] Introducing "dynamic crosslinking" binders, which can repair broken links between polymer chains of binders during cycling. These binders contribute to the structural stability of AAMs and control SEI formation.[117–119] High-elastic binders also have the ability to address the challenges arising from volume expansion. For instance, the incorporation of polyrotaxane can effectively maintain the cohesion of crushed particles without causing disintegration.[120]

4. Apparent Interfaces between Electrode and SEs

In conventional LIBs, liquid electrolytes infiltrate the planar interface between electrodes and separator, forming rapid and stable Li^+ transport pathways. However, limited by the manufacturing technology, it is difficult to assemble the integrated SSLIBs directly which means the inherent existence of electrode/SEs interface. Hence, an in-depth understanding on the design of apparent interfaces between electrode and SEs is critical to the construction of whole SSLIBs. However, the insufficient mechanical and electrochemical stability of the electrode/SE interface will inevitably lead to undesirable side reactions or poor physical contact, resulting in inferior rate performance and capacity retention.

4.1. Apparent Interfaces Between Composite Cathode and SEs

The concerning interfacial stability contributes to the decomposition of CAMs and SEs at high-voltage. Undesirable e^- transfer between the composite cathode/SEs interface will trigger chemical reaction and the resulting formation of the inactive decomposition interlayers (i.e., La_2O_3 and Li_2S), and even phase change and structural disordering of CAMs, all of which will increase the interfacial resistance (**Figure 9A**). As a consequence, the stable and carrier transport ordering interface between composite cathode and SEs plays vital roles to obtain the excellent performance of SSLIBs.

4.2. Apparent Interfaces Between Composite Anode and SEs

Different from cathode materials, strong mechanical property is especially vital for the composite anode/SEs interface except for the prerequisite electrochemical stability. On the one hand, alloy-type anodes (e.g., Si and Sn) are accompanied with huge and anisotropic swelling during the lithiation process, which results to stress evolution and fracture on the interface, eventually causing the degeneration of ionic conduction network (Figure 9B). On

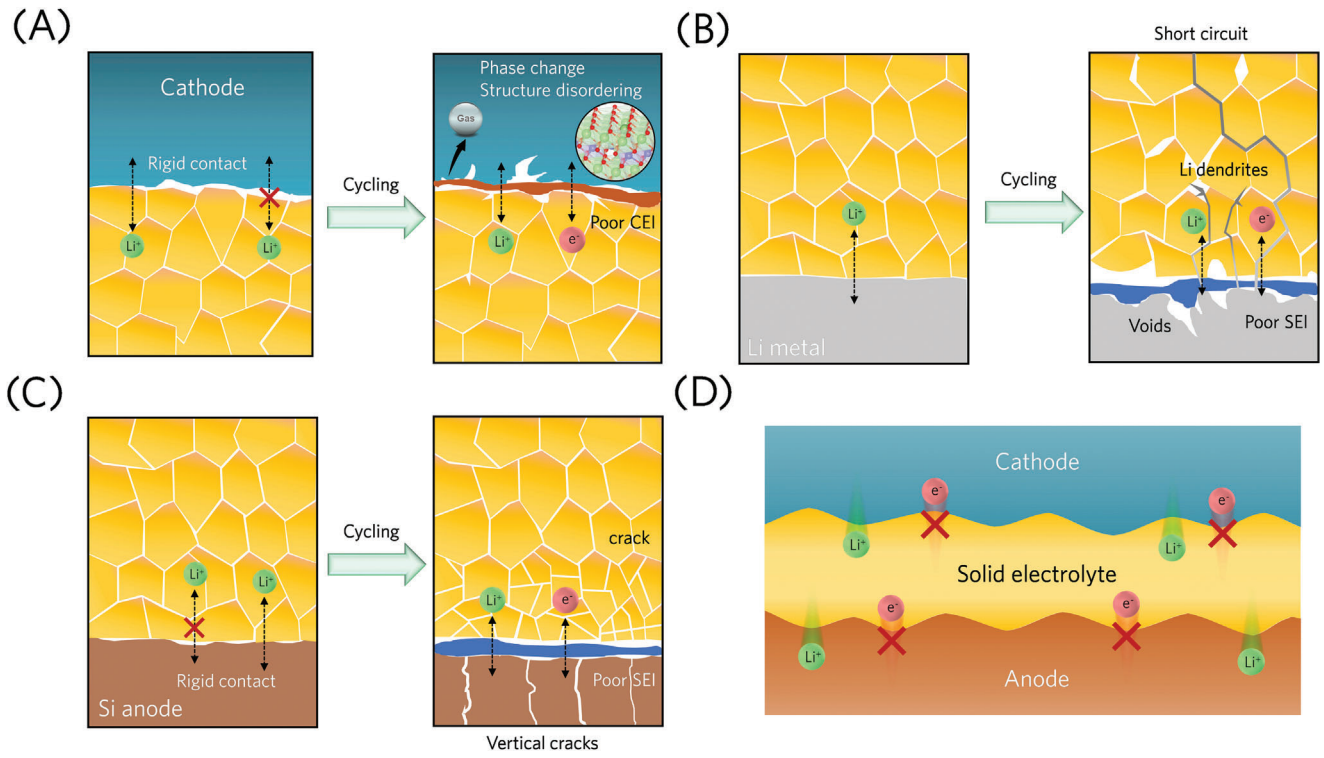

Figure 9. A) Schematic illustration of interface issues between composite cathode and SEs. B) Schematic illustration of interface issues between Li metal anode and SEs. C) Schematic illustration of interface issues between composite Si anode and SEs. D) Schematic illustration of ideal interfaces between electrodes and SEs.

the other hand, instability contact of interface, growth of lithium dendrites, and drastic side reactions with SEs shorten the life span of Li-metal anodes based on SSLIBs (Figure 9C). Essentially, Li^+ transport and Li deposition processes occur at the Li/SEs interface during cycling which needs to deeply understand the kinetics and failure mechanism. The ideal apparent interfaces between composite electrodes and SEs (Figure 9D) need to be regulated rationally to create a selective carrier transport network, inhibiting e^- transfer and accelerating Li^+ transfer.

4.3. Rigid Surface Contact

The rigid contact of electrodes and SEs interface often leads to a limited contact area, resulting in high interface contact impedance, the reduction of Li^+ pathways and accumulation of stress. Usually, most SEs add high external stacking pressure to maintain close contact with electrode materials during operation. Overall, there are two different ways to improve the rigid surface contact of composite cathode and SE: (1) The compressibility of SEs plays a crucial role in determining the extent of electrode/SE contact. A higher compressibility enables the SE to effectively cover a larger surface area of the AMPs when subjected to pressure. Consequently, the level of surface contact between the electrodes and SEs will improve. Oxychloride SE like $Li_{1.75}ZrCl_{4.75}O_{0.5}$ (LZCO) was found to have the ability to reach a density of 94.2% under 300 MPa.[121] Selecting these high-compressibility SEs applies sufficient pressure during the fabrication of a cold-pressed pellet, which can establish a more intimate and adequate connection between two surfaces (**Figure 10A**). (2) Alternatively, utilizing polymers such as PEO[122,123] and PVDF[124,125] to fabricate flexible composite solid electrolytes (SEs) can facilitate a "soft contact" between interfaces. This approach not only reduces polarization effects but also promotes chemically homogeneous lithium plating and stripping on the Li metal anode (Figure 10B). However, components used to apply pressure can reduce energy density, and the battery pack imposes strict upper limits on the pressure exerted on the battery stack. In order to achieve pressure-free SSLIBs, the design of SEs that possess viscoelastic properties akin to polymers can be used.[126] In pressure-free conditions, this lets them withstand deformation while also allowing the electrolyte to effectively permeate the electrode material and form a wetting interface.

4.4. Li^+ Diffusion Between SE and Li Metal

Metal ions in the electrolyte are deposited and crystallized into metal particles during electrochemical deposition.[127] The energy barrier of crystallization is an important factor contributing to electrochemical deposition overpotential.[128] High overpotential or polarization will result in low power density, low energy efficiency, and even battery failure. Classical nucleation theory defines the proliferation of metal particle nuclei during metal plating in liquid electrolytes.[129] To reveal the Li metal crystallization mechanisms during electrochemical plating in SSLIBs, recent studies used large-scale molecular dynamics simulations demonstrate that lithium crystallization occurs in multi-step routes

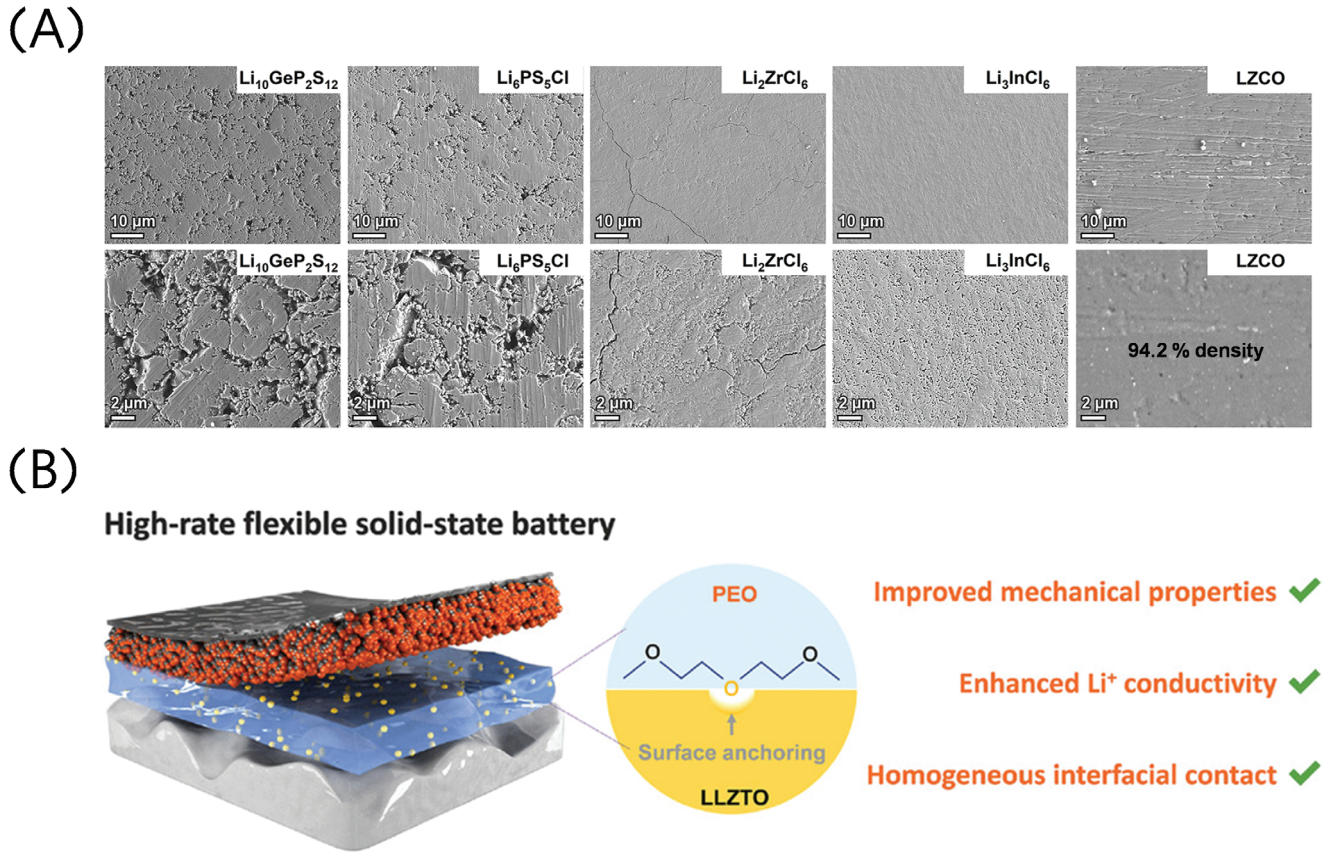

Figure 10. A) SEM images for the cold-pressed pellets of $Li_{10}GeP_2S_{12}$, Li_6PS_5Cl, Li_2ZrCl_6, Li_3InCl_6, and LZCO. All the pellets were fabricated under 300 MPa. Reproduced with permission.[121] Copyright 2023, Springer Nature. B) Working mechanisms for LLZTO with defective PEO in SSLIBs.[123]

mediated by interfacial lithium atoms with disordered and random-closed packed configurations as intermediate steps, giving rise to the crystallization energy barrier (**Figure 11**A). These intermediates in the crystallization pathways (interfacial atom states) are direct outcomes of the interfacial interactions between Li metal and SE and can therefore be modified via previously stated interface engineering strategies.[130]

In addition, the formation of voids and contact loss on the Li/SEs interface could happen during electrochemical cycling. When the striping current density moves the Li^+ away from the Li metal surface faster than it could be replenished, voids formed and accumulated during cycling, which would introduce localized concentrated current density and trigger the formation of lithium dendrites, leading to an increasing of interfacial resistance and thus restricting the rate capability of Li metal anode.[131] Impurity phase during SEs synthesis[132] and phase change of the SEs on contact with Li metal or during electrochemical process could also contribute to sluggish ionic transfer on the Li/SEs interface.

Dendrite and voids formed at the interface between Li and SE will result in a large interfacial resistance that prevents Li^+ diffusion on the surface.[133] Recent studies have demonstrated that coatings such as $Li_4Ti_5O_{12}$ (LTO) and polyaniline layers significantly regulate Li^+ distribution and deposition behavior, effectively suppressing the formation of dendrites and voids.[134,135] Furthermore, appropriate stack pressure was proven to suppress void formation,[136] but it cannot inhibit dendrite growth totally. In that case, the interface engineering strategy might be the ideal way to solve these problems, which can decrease the large interfacial resistance efficiently and hence increase the ionic diffusion on the Li/SEs interface: (1) Cleaning the impurity layer (Li_2CO_3 and Li_2O) on Li metal surface[137] and the SEs surface[138,139] and understanding the mechanism by which surface chemistry controls the resistance of the Li/SEs interface then enhances the wettability and achieves very low interfacial resistances (Figure 11B). (2) Adopting the alloying Li metal strategy, which enables intimate contact between the Li metal anode and SEs to show higher lithium diffusion coefficients than pure lithium[140,141] and reducing pore formation at the interface that significantly decreases the interface resistance.[142–146] (3) Introducing artificial wettability (MoS_2[147] and graphite[148]), wetting the interface with lean liquid electrolyte[149,150] and nano-wetted interfaces,[151–155] these methods will enhance the interface contact and promote uniform plating and stripping, resulting in improved ability to prevent the development and growth of dendrites (Figure 11C).

However, The presence of Si particles reduces the length of the diffusion channel in the composite electrode, making it more efficient.[156] The extensive contact area between Si particles and SEs as well as conductive agents allows for the efficient conduction of e^- and ions throughout the whole composite electrode.[157] This enhances the CCD of the anode and promotes the diffusion of AMPs. On the other hand, Li metal has smaller surface area

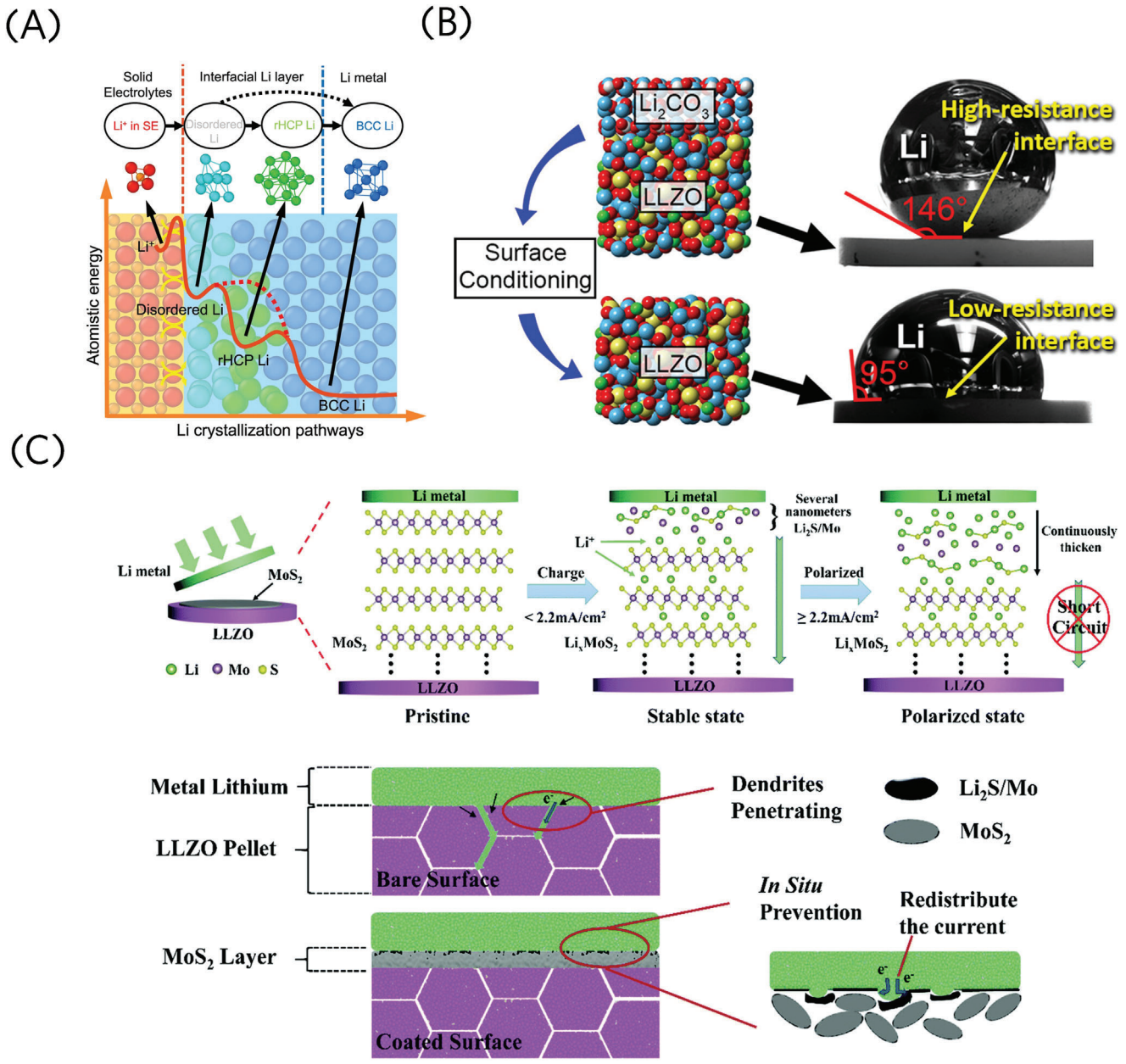

Figure 11. A) Multiple-step pathway of Li crystallization in SEs. Reproduced with permission.[130] Copyright 2023, Springer Nature. B) Schematic illustration of Li_2CO_3 layer impact on the interfacial resistance. Reproduced with permission.[138] Copyright 2017, American Chemical Society. C) Schematic diagrams of the in situ MoS_2 protection mechanism and its chemical evolution during the polarization process. Reproduced with permission.[147] Copyright 2019, Royal Society of Chemistry.

in contact with SEs, resulting in the limited CCD. In summary, the Si anode demonstrates superior compatibility with SSLIBs in comparison to the Li metal anode.

4.5. Chemical and Electrochemical Stability

The interface between the composite cathode and SEs was complicated, owing to elements diversity and the strong oxidization of the transition metal under high potential at charged state. Undesirable e^- transfer on the composite cathode and SE interface will trigger chemical reaction of both the cathodes and SEs. Density functional theoretical (DFT) calculation results have shown that most SEs will decompose beyond 5 V (vs Li/Li^+).[158,159] Garnet-type LLZO is found to have continuous irreversible reactions on the interface of LLZO/$LiMn_{1.5}Ni_{0.5}O_4$.[160] Argyrodite Li_6PS_5Cl is reported to be oxidized into elemental sulfur, phosphates, LiCl and lithium polysulfides, P_2S_x ($x \geq 5$) when matched with $LiCoO_2$, $LiNi_{1/3}Co_{1/3}Mn_{1/3}O_2$, and $LiMn_2O_4$.[161] Sulfide-based SEs such as LGPS would also undergo

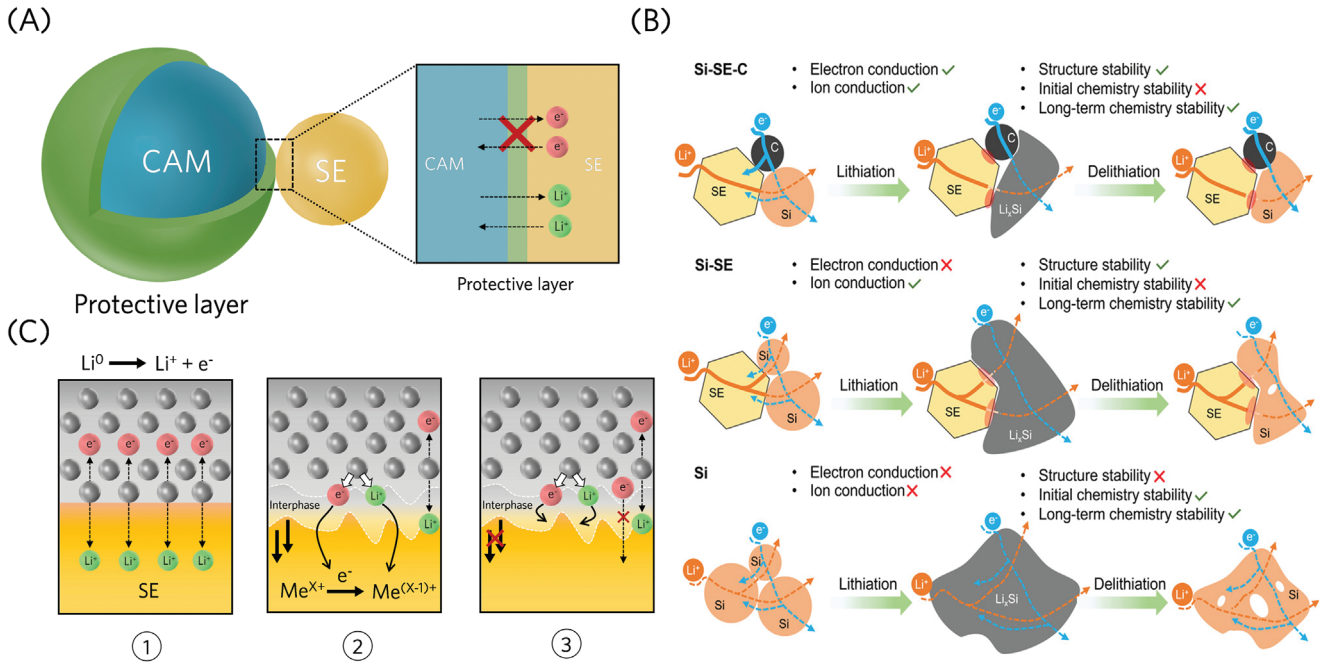

Figure 12. A) Schematic of interface stabilization with protective layer. B) Schematic illustration of the chemistry and structure evolution for various anodes in SSLIBs.[182] C) Three types of interfaces between Li metal and a solid lithium ion conductor. Reproduced with permission[183] Copyright 2015, Elsevier.

interfacial instability problems on the composite cathode/SE. The chemical reaction between LGPS and $LiNi_{0.8}Co_{0.15}Al_{0.05}O_2$ occurs immediately once contacted.[162] The LGPS will decompose into highly oxidized sulfur species, which can be accelerated by conductive carbon additives.[163] While the decomposition interlayers retard the ionic diffusion, the positive electrodes will undergo surface structural reconstruction.[164] The decomposition on the interface of the composite cathode materials and electrolytes under high-voltage will consume active Li^+, the inactive species will introduce high interfacial resistance, which will cause severely decay of the battery performances.[165] Many efforts have been devoted to increasing the interfacial stability on the composite cathode and SEs interface, one of the most efficient strategies is introducing a interface modification layer while chemical stable and compatible versus SEs, such as $Li_{0.35}La_{0.5}Sr_{0.05}TiO_3$,[166] $LiNbO_3$,[167,168] Li_3PO_4,[169–171] Al_2O_3,[172] $Li_4Ti_5O_{12}$,[173] $LiCO_3$,[174] Li_2SiO_3,[175] lithium zirconium oxides,[176] Li_3BO_3,[177] $LiTaO_3$[178] and diamond-like carbon (**Figure 12A**).[179] The interface modification layer with high ionic conductivity and very low e^- conductivity can promote interface contact, minimize interface resistance between different layers, and finally prevent detrimental side reactions.[180] Besides, it is imperative for this layer to possess a low lattice mismatch in order to avert the detachment of the buffer layer during the processes of charging and discharging.[181] It is worth mentioning that other strategies, such as the physical methodologies outlined in the preceding section, are insufficient for addressing the chemical stability issue at its root. Therefore, the most optimal strategy should still be the introduction of an interfacial modification layer.

As we mentioned before, due to the low electronic conductivity of Si particle itself, in that case, a certain amount of conductive agents (e.g., acetylene black) and SEs are mixed together to build the e^- and Li^+ conduction pathways in the AAMs, which enable good e^- and Li^+ accessibility to the AAMs then guarantee the double conductive network.[184] Additionally, it has the capability to restrict the significant increase in volume and prevent degradation and detachment. However, past researches have indicated that sulfide SEs tend to be unstable at the anode.[185,186] The presence of carbon can expedite the degradation of these SEs,[187] and the degree of decomposition is influenced by the specific kind of carbon material employed.[163] Therefore, carbon conductive agents tend to promote undesirable side reactions between SEs and Si and between SEs and carbon, leading to the chemistry change in AAMs during electrochemical reactions (Figure 12B).[182]

In any case, the ion/electron percolation in the AAMs suffers from these decomposition reactions. This leads to heightened resistance for Li^+ and e^-, ultimately resulting in the capacity decline in SSLIBs. However, apart from carbon additive, varying SEs have different chemical and electrochemical stability with Si anodes.[188] The major cause of side reactions between sulfide-based SEs and Si particles is the interaction between Si and P. Hydride-based SEs, such as $3LiBH_4$-LiI (LBHI), have exceptional electrochemical stability when used with Si anodes.[189] They do not show any noticeable electrochemical degradation as compared to sulfide-based SE.

Additionally, the substantial fluctuations in volume of the Si particles throughout their cycling give rise to the unstable SEI layer, which is referred to as "dynamic SEI reconstruction." Si-based SSLIBs eventually develop a dense SEI layer, hence an irreversible capacity loss.[190] To achieve the desired interfacial and mechanical stability, a low mobility poly(vinylidene fluoride-co-hexafluoropropylene) was used to form a flow-domain SEI rich

Table 1. Summary of various interfacial engineering strategies.

Interfacial engineering		Strategies
Internal Interfaces within SEs	Electron conduction × Ionic conduction ✓	*Grain-boundary electronic insulation* (Choosing electronic insulation materials with low electronic conductivity and high humidity stability) *Isotropic glass additions* (Introducing additions with good wetting properties to coat the pores and fill the grain) *Heating densification* (Controlling the size and orientation of the grains)
Internal Interfaces within Electrode	Electron conduction ✓ Ionic conduction ✓	*Electrode architecture design* (Promoting direct atomic-level contact between the AMPs and enable the formation of nano-wetted interfaces) *Void filling media* (Facilitating interfacial contact between SEs and the AMPs) *Conductive binders* (Bridging the gap between the ion conductive network and electronic conductive network in molecular-level) *Thermal sintering* (Promotes the fusion of the SE and AMPs interfaces while preventing unwanted phase diffusion) *External pressure* (Restricting AMPs volume expansion and cracking)
Apparent Interfaces between Electrode and SEs	Electron conduction × Ionic conduction ✓	*Multifunctional interface layer* (Introducing protection layer with high ionic conductivity and electronic insulation abilities) *Flexible composite SEs* (Reducing the polarization effects and enabling homogeneous lithium plating/stripping on the Li metal anode) *Impurity layer cleaning* (Enhancing the wettability and lowering interfacial resistances) *Li-containing alloy* (Enabling intimate contact between the Li metal anode and SEs reducing pore formation at the interface)

in LiF.[110] In addition, a hard-carbon-stabilized Li-Si alloy AAMs is constructed, and a 3D fast ionic-electronic conducting network including Li-rich phases ($Li_{15}Si_4/LiC_6$) is generated inside the ACE to form stable SEI, enlarging the active region and relieving stress concentration, resulting in better electrode kinetics and mechanical stability.[191] 99.9 wt % pristine micro-silicon (μSi) and 0.1% PVDF were also introduced to construct a pure Si anode. Removing carbon conductive additives from the anode can reduce SEs decomposition and unwanted side reactions, which effectively prevents drop in capacity. Concurrently, the μSi particles form a stable SEI interface and a direct link between Li^+ and e^-, enabling rapid diffusion of Li^+ and efficient e^- transport throughout the electrode.[187]

The electrochemical window and the stability of the SSLIBs not only relied on the intrinsic electrochemical stability of the electrolytes but also on the compatibility or the interfacial stability between electrolytes and electrodes. First-principles computation methods were employed to investigate the electrochemical stability of the interface.[159,192] The phase equilibria and decomposition reaction energies of lithiation (delithiation) of the SEs were calculated and compared. In contrast to widely perception of the stability of SEs, most of the SEs had a limited intrinsic electrochemical and would form thermodynamically favorable decomposition interfaces either at low or high potentials at interface. These formed interphase layers with different chemical properties, which could be categorized into three typical interfaces: (1) Stable interface with negligible side reaction; (2) Formation of a mixed (ionic/electronic) conducting interphase (MCI); (3) Formation of SEI with ionic conductivity and electronic insulation.

Since the first type of interface is unrealistic and the second type is not stable, constructing an interphase that only "filters out" electrons is the only choice. In some cases, the SE would undergo spontaneous but not continuous decomposition, for example, decomposition interface composed of Li_3PO_4, Li_3P, Li_3N and Li_2O would form when $Li_6P_3O_9N$ (LiPON) on contact with Li metal.[193] Once the electrochemically insulating interface layers form, the electrolyte interface would be passivated and remained stable during the electrochemical cycling. Different interface engineering strategies were developed to construct a stable interphase. For example, introduction of protection layer with high ionic conductivity and electronic insulation abilities via *ex/in-situ* reaction,[194] coating layer on the SEs (MoS_2,[195] Si,[196] LiF[197] or LiI,[198] Al_2O_3,[199] amorphous Ge thin film,[200] boron nitride,[201] ZnO,[202] chromium,[203] gel polymer modification,[204–206]) increasing the contact areal by three-dimensional SEs,[207] which can improve chemical and electrochemical stability significantly (Figure 12C).

5. Outlook and Perspective

Compared with conventional liquid-based LIBs, SSLIBs stand out because of their potential high energy density and outstanding safety. As demonstrated in the previous literature, the multiple scales solid-solid interfaces play a key role in SSLIBs, controlling the transportation of carriers. These solid-solid interfaces include three internal interfaces (composite cathode, SEs and composite anode) and two apparent interfaces between composite cathode/anode and SEs, frequently acting as the bottleneck for the overall carrier transport whose properties are quite

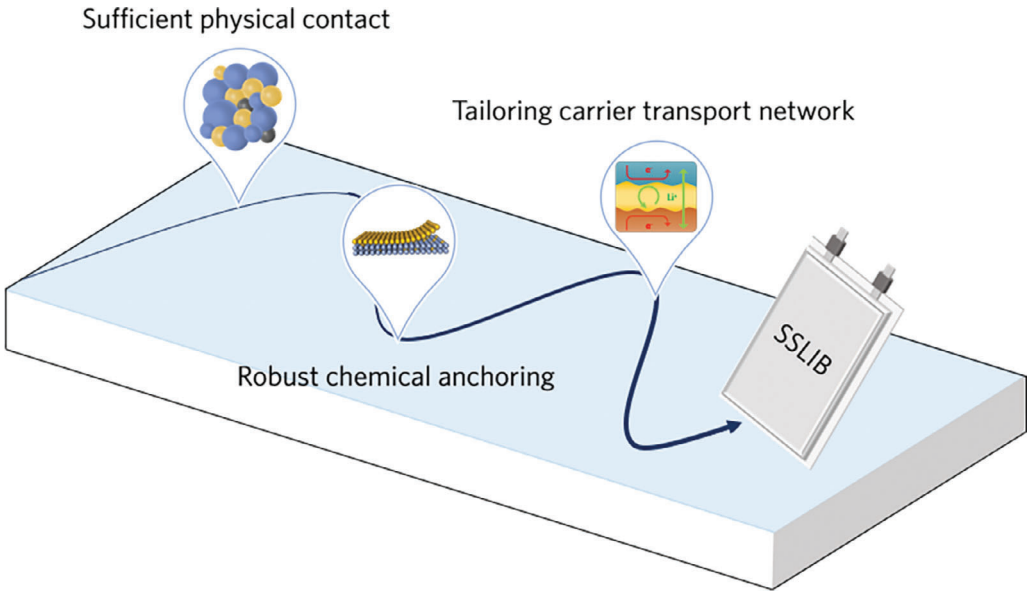

Figure 13. Perspectives for the design guideline of future SSLIBs.

different from those of percolative liquid-solid interfaces. For example, GBs in SEs impedes the Li^+ transport generally, even leading to the poor mechanical property. The unstable point-contact of solid-solid interfaces would result in large interfacial resistance and considerable capacity loss SSLIBs. For ideal internal interfaces, Li^+ and e^- are transported cooperatively in the composite electrode. On the contrary, desired SEs exhibit the high ionic conductivity and extremely low electronic conductivity even insulation. It is worth noting that electron transfer should also be suppressed at the electrode/SEs interface to avoid side reactions. A robust conductive carrier network should be tailored and constructed in SSLIBs via interfacial engineering. **Table 1** provides a concise overview of the interfacial modification strategies discussed in this review.

Although remarkable achievements have been made on the interfacial issues, there is still a bumpy way for SSLIBs commercialization. Combining the above, the optimization strategies and design principles of SSLIBs are summarized in **Figure 13**. Most fundamentally, sufficient physical contact of each solid component (e.g., active material particles, electronic conductive agents and SEs) is the cornerstone for carrier transport and battery operation. Secondly, constructing a robust chemical anchoring among the multiple scales solid-solid interfaces to maintain the physical contact during cycling is vital for batteries especially for the system with large volume changes. On this basis, establishing the in-depth understanding of Li^+ and e^- transport and tailoring the selective carrier transport network in the whole SSLIBs is crucial for addressing the prevailing problems associated with interfaces, which involve complex physical, (electro)chemical, and electrochemical-mechanical processes. The following paragraphs describe the future challenges and research directions needed to accelerate the practical application of SSLIBs.

1) Increasing the ratio of active materials in practical cells through rational electrode design shows great potential to achieve higher energy density of SSLIBs. However, increasing electrode thickness leads to the longer carrier transport distances, resulting in poor charge transfer kinetics and ion-concentration gradient along the longitudinal axis. This issue could be improved by introducing solid polymer electrolytes, applying multi-dimensional conductive additives (e.g., carbon nanotubes and graphene), and matching the size of the cathode material and electrolyte.
2) Scalable and economic manufacturing technologies are critical for the commercialization of SSLIBs. Traditional slurry-casting electrode fabrication technology often leads to cracking or delamination of thick electrodes and results in a higher tortuosity due to the random arrangement of particles, hindering rapid carrier transport. One effective solution is to build the thick electrodes with vertical channels through template method or self-assembly strategies, decreasing the transport distance of Li^+/e^-. Additionally, solvent-free dry-film technologies, such as powder spray and binder fibrillation, deserve more attention in the future. These methods are not limited by electrode thickness and suppresses the delamination of various electrode components, constructing a favorable transport network. Designing robust multi-dimensional current collectors is an alternative path that could improve the Li^+ transport flux.
3) The design and synthesis of SEs with high ionic conductivities and wide electrochemical stability are essential for the development of high-performance SSLIBs. Oxide-based SEs face challenges such as high GB resistance and excessive hardness due to the inherent properties of materials, leading to the poor contact. In this aspect, halide-based SEs and sulfide-based SEs are more promising due to their better ionic conductivity and ductility. Moreover, developing thin electrolyte layer fabrication technology is also important for the manufacturing of practical SSLIBs.
4) On the cathode side, severe physical contact issues and high-voltage instability condition are significant problems

that need further consideration. Developing a soft and ion-conducting coating layer for CAMs and regulating the 3D structure for the electrode may alleviate these issues. For the anode side, more attention should be paid for how to restrain the growth of Li dendrite and suppress the volume variation during cycling. Constructing multilayer and dynamically stable interfaces, employing self-healing and ion-electron conducting binders, and designing external applied pressure devices for pouch cells have potential to address these challenges.

5) Advanced in situ characterization techniques (e.g., in situ X-ray photoelectron spectroscopy, in situ NMR spectroscopy and in situ TEM) should be developed to deeply understand the complicated evaluation mechanisms of the composition and structure on the interface, guiding the rational design of interfacial structure of SSLIBs.[208–210] For instance, operando X-ray computed tomography has been employed to observe the growth of lithium dendrite in real time. However, a limited number of electrode materials have been investigated by these advanced characterization strategies which also requires specific equipment for experiments.
6) Theoretical calculation and simulation (e.g., density functional theory calculation, molecular dynamics simulation and finite element simulation) are powerful tools to screen promising SEs and analyze the physicochemical processes in SSLIBs.[211] Through calculating the properties (e.g., electrochemical window and ion transport) of SEs, large computational materials database could be established. Besides, it is significant to develop the multi-scale simulation models (from materials to batteries), forecasting the electrochemical behavior and stress distribution in SSLIBs.[212–215]

With this review, we hope to stimulate research in these directions to further achieve high performance SSLIBs. After establishing a selective and stable carrier transport network in the entire solid-state batteries, the commercialization of SSLIBs could be around the corner.

Acknowledgements

Z.D. and S.C. contributed equally to this work. F.P. acknowledges the support from International joint Research Center for Electric Vehicle Power Battery and Materials (No. 2015B01015), Guangdong Key Laboratory of Design and calculation of New Energy Materials (No. 2017B030301013) and the Shenzhen Key Laboratory of New Energy Resources Genome Preparation and Testing (No. ZDSYS201707281026184). L.Y. acknowledges the support from Shenzhen Science and Technology Planning Project (JSGG20220831095604008). Y.S. acknowledges the support from the National Natural Science Foundation of China (No. 52102200).

Conflict of Interest

The authors declare no conflict of interest.

Keywords

apparent electrode/SEs interfaces, carrier transport network, internal interfaces, solid-state lithium-ion batteries

Received: June 4, 2024
Revised: July 17, 2024
Published online: July 31, 2024

[1] L. Han, Z. Wang, D. Kong, L. Yang, K. Yang, Z. Wang, F. Pan, *J. Mater. Chem. A* **2018**, *6*, 21280.
[2] K. Xu, *Chem. Rev.* **2004**, *104*, 4303.
[3] K. Xu, *Chem. Rev.* **2014**, *114*, 11503.
[4] X. Cheng, M. Zhao, C. Chen, A. Pentecost, K. Maleski, T. Mathis, X. Zhang, Q. Zhang, J. Jiang, Y. Gogotsi, *Nat. Commun.* **2017**, *8*, 336.
[5] Z. Wang, F. Zhang, Y. Sun, L. Zheng, Y. Shen, D. Fu, W. Li, A. Pan, L. Wang, J. Xu, J. Hu, X. Wu, *Adv. Energy Mater.* **2021**, *11*, 2003752.
[6] Y. Wu, D. Ren, X. Liu, G. L. Xu, X. Feng, Y. Zheng, Y. Li, M. Yang, Y. Peng, X. Han, L. Wang, Z. Chen, Y. Ren, L. Lu, X. He, J. Chen, K. Amine, M. Ouyang, *Adv. Energy Mater.* **2021**, *11*, 2102299.
[7] H. Zhang, L. Wang, X. He, *Battery Energy* **2022**, *1*, 20210011.
[8] Z. Zhu, T. Jiang, M. Ali, Y. Meng, Y. Jin, Y. Cui, W. Chen, *Chem. Rev.* **2022**, *122*, 16610.
[9] D. H. S. Tan, A. Banerjee, Z. Chen, Y. S. Meng, *Nat. Nanotechnol.* **2020**, *15*, 170.
[10] Q. Zhao, S. Stalin, C. Z. Zhao, L. A. Archer, *Nat. Rev. Mater.* **2020**, *5*, 229.
[11] A. Manthiram, X. Yu, S. Wang, *Nat. Rev. Mater.* **2017**, *2*, 16103.
[12] S. Li, S. Q. Zhang, L. Shen, Q. Liu, J. Bin Ma, W. Lv, Y. B. He, Q. H. Yang, *Adv. Sci.* **2020**, *7*, 190308.
[13] Z. Liao, S. Zhang, Y. Zhao, Z. Qiu, K. Li, D. Han, G. Zhang, T. G. Habetler, *J. Energy Chem.* **2020**, *49*, 124.
[14] Y. Wu, S. Wang, H. Li, L. Chen, F. Wu, *InfoMat* **2021**, *3*, 827.
[15] S. Randau, D. A. Weber, O. Kötz, R. Koerver, P. Braun, A. Weber, E. Ivers-Tiffée, T. Adermann, J. Kulisch, W. G. Zeier, F. H. Richter, J. Janek, *Nat. Energy* **2020**, *5*, 259.
[16] T. Liu, Y. Zhang, R. Chen, S. X. Zhao, Y. Lin, C. W. Nan, Y. Shen, *Electrochem. Commun.* **2017**, *79*, 1.
[17] B. He, F. Zhang, Y. Xin, C. Xu, X. Hu, X. Wu, Y. Yang, H. Tian, *Nat. Rev. Chem.* **2023**, *7*, 826.
[18] E. Quemin, R. Dugas, T. Koç, B. Hennequart, R. Chometon, J. M. Tarascon, *ACS Appl. Mater. Interfaces* **2022**, *14*, 49284.
[19] X. Zhang, Q. Xiang, S. Tang, A. Wang, X. Liu, J. Luo, *Nano Lett.* **2020**, *20*, 2871.
[20] C. Zheng, Y. Lu, J. Su, Z. Song, T. Xiu, J. Jin, M. E. Badding, Z. Wen, *Small Methods* **2022**, *6*, 220667.
[21] J. A. Quirk, J. A. Dawson, *Adv. Energy Mater.* **2023**, *13*, 2301114.
[22] V. A. Online, K. Chen, C. Liang, C. Nan, R. Ishikawa, K. More, M. Chi, *Energy Environ. Sci.* **2014**, *7*, 1638.
[23] L. Al, P. O. Ge, C. R. Mariappan, M. Gellert, C. Yada, F. Rosciano, B. Roling, *Electrochem. Commun.* **2012**, *14*, 25.
[24] C. Zhu, T. Fuchs, S. A. L. Weber, F. H. Richter, G. Glasser, F. Weber, H. J. Butt, J. Janek, R. Berger, *Nat. Commun.* **2023**, *14*, 1300.
[25] A. Banerjee, X. Wang, C. Fang, E. A. Wu, Y. S. Meng, *Chem. Rev.* **2020**, *120*, 6878.
[26] X. Miao, H. Wang, R. Sun, C. Wang, Z. Zhang, *Energy Environ. Sci.* **2020**, *13*, 3780.
[27] R. Murugan, V. Thangadurai, W. Weppner, *Angew. Chem. – Int. Ed.* **2007**, *46*, 7778.
[28] L. Chen, W. Zhang, Z. Nie, S. Li, F. Pan, *J. Mater. Inform.* **2021**, *1*, 4.
[29] C. R. Mariappan, M. Gellert, C. Yada, F. Rosciano, B. Roling, *Electrochem. Commun.* **2012**, *14*, 25.
[30] Q. Xu, C. L. Tsai, D. Song, S. Basak, H. Kungl, H. Tempel, F. Hausen, S. Yu, R. A. Eichel, *J. Power Sources* **2021**, *492*, 229631.
[31] S. Stegmaier, R. Schierholz, I. Povstugar, J. Barthel, S. P. Rittmeyer, S. Yu, S. Wengert, S. Rostami, H. Kungl, K. Reuter, R. A. Eichel, C. Scheurer, *Adv. Energy Mater.* **2021**, *11*, 2100707.

[32] Y. Luo, H. Gao, X. Zhao, *Ceram. Int.* **2022**, *48*, 8387.
[33] D. K. Singh, A. Henss, B. Mogwitz, A. Gautam, J. Horn, T. Krauskopf, S. Burkhardt, J. Sann, F. H. Richter, J. Janek, *Cell Reports Phys. Sci.* **2022**, *3*, 101043.
[34] A. Shara, C. G. Haslam, *J. Mater. Chem. A.* **2017**, *5*, 21491.
[35] Y. Zhu, S. Wu, Y. Pan, X. Zhang, Z. Yan, Y. Xiang, *Nanoscale Res. Lett.* **2020**, *15*, 153.
[36] A. Mei, X. L. Wang, J. Le Lan, Y. C. Feng, H. X. Geng, Y. H. Lin, C. W. Nan, *Electrochim. Acta.* **2010**, *55*, 2958.
[37] H. Moriwake, X. Gao, A. Kuwabara, C. A. J. Fisher, T. Kimura, Y. H. Ikuhara, K. Kohama, T. Tojigamori, Y. Ikuhara, *J. Power Sources* **2015**, *276*, 203.
[38] H. Zhang, S. Hao, J. Lin, *J. Alloys Compd.* **2017**, *704*, 109.
[39] K. Kwatek, W. Ślubowska, J. Trébosc, O. Lafon, J. L. Nowiński, *J. Alloys Compd.* **2020**, *820*, 153072.
[40] T. Thompson, A. Sharafi, M. D. Johannes, A. Huq, J. L. Allen, J. Wolfenstine, J. Sakamoto, *Adv. Energy Mater.* **2015**, *5*, 150096.
[41] K. Zhang, T. Xu, H. Zhao, *Int. J. Energy Res.* **2020**, *44*, 9177.
[42] H. Yamada, T. Ito, R. H. Basappa, *Electrochim. Acta* **2016**, *222*, 648.
[43] M. Kotobuki, B. Kobayashi, M. Koishi, T. Mizushima, N. Kakuta, *Mater. Technol.* **2014**, *29*, A93.
[44] M. Kotobuki, M. Koishi, *J. Asian Ceram. Soc.* **2020**, *8*, 891.
[45] J. Leng, H. Liang, H. Wang, Z. Xiao, S. Wang, Z. Zhang, Z. Tang, *Nano Energy* **2022**, *101*, 107603.
[46] H. Zhou, Y. Zhou, X. Li, X. Huang, B. Tian, *ACS Appl. Mater. Interfaces* **2024**, *16*, 5989.
[47] C. Wang, K. Fu, S. P. Kammampata, D. W. McOwen, A. J. Samson, L. Zhang, G. T. Hitz, A. M. Nolan, E. D. Wachsman, Y. Mo, V. Thangadurai, L. Hu, *Chem. Rev.* **2020**, *120*, 4257.
[48] G. V. Alexander, M. S. Indu, R. Murugan, *Ionics* **2021**, *27*, 4105.
[49] M. J. Counihan, D. J. Powers, P. Barai, S. Hu, T. Zagorac, Y. Zhou, J. Lee, J. G. Connell, K. S. Chavan, I. S. Gilmore, L. Hanley, V. Srinivasan, Y. Zhang, S. Tepavcevic, *ACS Appl. Mater. Interfaces* **2023**, *15*, 26047.
[50] B. Gao, R. Jalem, H. K. Tian, Y. Tateyama, *Adv. Energy Mater.* **2022**, *12*, 2102151.
[51] Y. Song, L. Yang, L. Tao, Q. Zhao, Z. Wang, Y. Cui, H. Liu, Y. Lin, F. Pan, *J. Mater. Chem. A* **2019**, *7*, 22898.
[52] X. Yang, X. Gao, M. Jiang, J. Luo, J. Yan, J. Fu, H. Duan, S. Zhao, Y. Tang, R. Yang, R. Li, J. Wang, H. Huang, C. Veer Singh, X. Sun, *Angew. Chem. – Int. Ed.* **2023**, *62*, e202215680.
[53] Y. Song, L. Yang, W. Zhao, Z. Wang, Y. Zhao, Z. Wang, Q. Zhao, H. Liu, F. Pan, *Adv. Energy Mater.* **2019**, *9*, 1900671.
[54] F. Mo, J. Ruan, S. Sun, Z. Lian, S. Yang, X. Yue, Y. Song, Y. N. Zhou, F. Fang, G. Sun, S. Peng, D. Sun, *Adv. Energy Mater.* **2019**, *9*, 1902123.
[55] B. Xu, W. Li, H. Duan, H. Wang, Y. Guo, H. Li, H. Liu, *J. Power Sources* **2017**, *354*, 68.
[56] J. S. Kim, H. Kim, M. Badding, Z. Song, K. Kim, Y. Kim, D. J. Yun, D. Lee, J. Chang, S. Kim, D. Im, S. Park, S. H. Kim, S. Heo, *J. Mater. Chem. A* **2020**, *8*, 16892.
[57] S. Y. Ham, H. Yang, O. Nunez-cuacuas, D. H. S. Tan, Y. T. Chen, G. Deysher, A. Cronk, P. Ridley, J. M. Doux, E. A. Wu, J. Jang, Y. S. Meng, *Energy Storage Mater.* **2023**, *55*, 455.
[58] Y. Su, L. Ye, W. Fitzhugh, Y. Wang, E. Gil-González, I. Kim, X. Li, *Energy Environ. Sci.* **2020**, *13*, 908.
[59] L. Feng, Z. W. Yin, C. W. Wang, Z. Li, S. J. Zhang, P. F. Zhang, Y. P. Deng, F. Pan, B. Zhang, Z. Lin, *Adv. Funct. Mater.* **2023**, *33*, 2210744.
[60] C. Li, Y. Wu, Z. Lv, J. Peng, J. Liu, X. Zheng, Y. Wu, W. Tang, Z. Gong, Y. Yang, *Energy Mater.* **2024**, *4*, 400009.
[61] Z. Zeng, J. Cheng, Y. Li, H. Zhang, D. Li, H. Liu, F. Ji, Q. Sun, L. Ci, *Mater. Today Phys.* **2023**, *32*, 101009.
[62] Z. Wang, L. Yang, J. Liu, Y. Song, Q. Zhao, K. Yang, F. Pan, *ACS Appl. Mater. Interfaces* **2020**, *12*, 48677.
[63] K. Nie, Y. Hong, J. Qiu, Q. Li, X. Yu, H. Li, L. Chen, *Front. Chem.* **2018**, *6*, 616.
[64] S. H. Jung, U. H. Kim, J. H. Kim, S. Jun, C. S. Yoon, Y. S. Jung, Y. K. Sun, *Adv. Energy Mater.* **2020**, *10*, 1903360.
[65] G. L. Xu, Q. Liu, K. K. S. Lau, Y. Liu, X. Liu, H. Gao, X. Zhou, M. Zhuang, Y. Ren, J. Li, M. Shao, M. Ouyang, F. Pan, Z. Chen, K. Amine, G. Chen, *Nat. Energy* **2019**, *4*, 484.
[66] F. Aguesse, W. Manalastas, L. Buannic, J. M. L. Del Amo, G. Singh, A. Llordés, J. Kilner, *ACS Appl. Mater. Interfaces* **2017**, *9*, 3808.
[67] Y. Li, Y. Li, Y. Yang, Z. Cui, J. Wang, T. Zhang, *Chem. Commun.* **2020**, *56*, 1725.
[68] J. Sastre, X. Chen, A. Aribia, A. N. Tiwari, Y. E. Romanyuk, *ACS Appl. Mater. Interfaces* **2020**, *12*, 36196.
[69] W. Feng, Z. Lai, X. Dong, P. Li, Y. Wang, Y. Xia, *iScience* **2020**, *23*, 101071.
[70] S. Ohta, T. Kobayashi, J. Seki, T. Asaoka, *J. Power Sources* **2012**, *202*, 332.
[71] X. Zhu, T. Zhao, P. Tan, Z. Wei, M. Wu, *Nano Energy* **2016**, *26*, 565.
[72] K. Fu, Y. Gong, G. T. Hitz, D. W. McOwen, Y. Li, S. Xu, Y. Wen, L. Zhang, C. Wang, G. Pastel, J. Dai, B. Liu, H. Xie, Y. Yao, E. D. Wachsman, L. Hu, *Energy Environ. Sci.* **2017**, *10*, 1568.
[73] X. B. Zhu, T. S. Zhao, Z. H. Wei, P. Tan, G. Zhao, *Energy Environ. Sci.* **2015**, *8*, 2782.
[74] X. B. Zhu, T. S. Zhao, Z. H. Wei, P. Tan, L. An, *Energy Environ. Sci.* **2015**, *8*, 3745.
[75] P. Minnmann, F. Strauss, A. Bielefeld, R. Ruess, P. Adelhelm, S. Burkhardt, S. L. Dreyer, E. Trevisanello, H. Ehrenberg, T. Brezesinski, F. H. Richter, J. Janek, *Adv. Energy Mater.* **2022**, *12*, 2201425.
[76] X. D. Zhang, F. S. Yue, J. Y. Liang, J. L. Shi, H. Li, Y. G. Guo, *Small Struct.* **2020**, *1*, 2000042.
[77] Z. Wang, R. Tan, H. Wang, L. Yang, J. Hu, H. Chen, F. Pan, *Adv. Mater.* **2018**, *30*, 1704436.
[78] D. S. Jolly, Z. Ning, J. E. Darnbrough, J. Kasemchainan, G. O. Hartley, P. Adamson, D. E. J. Armstrong, J. Marrow, P. G. Bruce, *ACS Appl. Mater. Interfaces* **2020**, *12*, 678.
[79] J. M. Doux, Y. Yang, D. H. S. Tan, H. Nguyen, E. A. Wu, X. Wang, A. Banerjee, Y. S. Meng, *J. Mater. Chem. A* **2020**, *8*, 5049.
[80] T. Demuth, T. Fuchs, F. Walther, A. Pokle, S. Ahmed, M. Malaki, A. Beyer, J. Janek, K. Volz, *Matter* **2023**, *6*, 2324.
[81] X. Yao, S. Chen, C. Wang, T. Chen, J. Li, S. Xue, Z. Deng, W. Zhao, B. Nan, Y. Zhao, K. Yang, Y. Song, F. Pan, L. Yang, X. Sun, *Adv. Energy Mater.* **2023**, *14*, 2303422.
[82] M. Rana, Y. Rudel, P. Heuer, E. Schlautmann, C. Rosenbach, M. Y. Ali, H. Wiggers, A. Bielefeld, W. G. Zeier, *ACS Energy Lett.* **2023**, *8*, 3196.
[83] R. Tan, J. Yang, J. Zheng, K. Wang, L. Lin, S. Ji, J. Liu, F. Pan, *Nano Energy* **2015**, *16*, 112.
[84] J. Yang, X. Kang, L. Hu, X. Gong, D. He, T. Peng, S. Mu, *J. Alloys Compd.* **2013**, *572*, 158.
[85] Y. Li, Y. Wu, T. Ma, Z. Wang, Q. Gao, J. Xu, L. Chen, H. Li, F. Wu, *Adv. Energy Mater.* **2022**, *12*, 2201732.
[86] D. Cao, Q. Li, X. Sun, Y. Wang, X. Zhao, E. Cakmak, W. Liang, A. Anderson, S. Ozcan, H. Zhu, *Adv. Mater.* **2021**, *33*, 2105505.
[87] S. B. Hong, Y. J. Lee, U. H. Kim, C. Bak, Y. M. Lee, W. Cho, H. J. Hah, Y. K. Sun, D. W. Kim, *ACS Energy Lett.* **2022**, *7*, 1092.
[88] T. J. Embleton, J. Yun, J. H. Choi, J. Kim, K. Ko, J. Kim, Y. Son, P. Oh, *Appl. Surf. Sci.* **2023**, *610*, 155490.
[89] J. E. Trevey, K. W. Rason, C. R. Stoldt, S. H. Lee, *Electrochem. Solid-State Lett.* **2010**, *13*, A154.
[90] R. Ma, Y. Fan, Y. Jin, S. Pan, H. Zhong, Y. Luo, J. Gu, M. Luo, Y. Wu, W. Hu, P. Chen, Y. Su, G. Wu, J. Yan, J. Gao, Z. Gong, Y. Yang, *Adv. Energy Mater.* **2024**, *14*, 2304412.

[91] A. Orue, J. M. López del Amo, F. Aguesse, M. Casas-Cabanas, P. López-Aranguren, *Energy Storage Mater.* **2023**, *54*, 524.
[92] X. Yang, K. Doyle-Davis, X. Gao, X. Sun, *eTransportation* **2022**, *11*, 100152.
[93] M. Kroll, S. L. Karstens, M. Cronau, A. Höltzel, S. Schlabach, N. Nobel, C. Redenbach, B. Roling, U. Tallarek, *Batter. Supercaps* **2021**, *4*, 1363.
[94] Z. Yan, L. Wang, H. Zhang, X. He, *Adv. Energy Mater.* **2024**, 2303206.
[95] J. C. Bachman, S. Muy, A. Grimaud, H. H. Chang, N. Pour, S. F. Lux, O. Paschos, F. Maglia, S. Lupart, P. Lamp, L. Giordano, Y. Shao-Horn, *Chem. Rev.* **2016**, *116*, 140.
[96] Z. Wang, X. Shen, S. Chen, R. Qiao, B. Sun, J. Deng, J. Song, *Adv. Mater.* **2024**, 2405025.
[97] Z. T. Sun, S. H. Bo, *J. Mater. Res.* **2022**, *37*, 3130.
[98] N. A. Dunlap, S. Kim, J. J. Jeong, K. H. Oh, S. H. Lee, *Solid State Ionics* **2018**, *324*, 207.
[99] T. Mu, Y. Zhao, C. Zhao, N. G. Holmes, S. Lou, J. Li, W. Li, M. He, Y. Sun, C. Du, R. Li, J. Wang, G. Yin, X. Sun, *Adv. Funct. Mater.* **2021**, *31*, 2010526.
[100] X. Han, M. Xu, L. H. Gu, C. F. Lan, M. F. Chen, J. J. Lu, B. F. Sheng, P. Wang, S. Y. Chen, J. Z. Chen, *Rare Met.* **2024**, *43*, 1017.
[101] D. M. Piper, T. A. Yersak, S.-H. Lee, *J. Electrochem. Soc.* **2013**, *160*, A77.
[102] J. Tao, J. Han, Y. Wu, Y. Yang, Y. Chen, J. Li, Z. Huang, Y. Lin, *Energy Storage Mater.* **2024**, *64*, 103082.
[103] M. Yamamoto, Y. Terauchi, A. Sakuda, M. Takahashi, *J. Power Sources* **2018**, *402*, 506.
[104] D. Cao, X. Sun, Y. Li, A. Anderson, W. Lu, H. Zhu, *Adv. Mater.* **2022**, *34*, 2200401.
[105] H. Pan, L. Wang, Y. Shi, C. Sheng, S. Yang, P. He, H. Zhou, *Nat. Commun.* **2024**, *15*, 2263.
[106] H. Huo, J. Janek, *ACS Energy Lett.* **2022**, *7*, 4005.
[107] L. Zhang, Y. Lin, X. Peng, M. Wu, T. Zhao, *ACS Appl. Mater. Interfaces* **2022**, *14*, 24798.
[108] Z. Xiao, C. Lei, C. Yu, X. Chen, Z. Zhu, H. Jiang, F. Wei, *Energy Storage Mater.* **2020**, *24*, 565.
[109] D. Wang, C. Zhou, B. Cao, Y. Xu, D. Zhang, A. Li, J. Zhou, Z. Ma, X. Chen, H. Song, *Energy Storage Mater.* **2020**, *24*, 312.
[110] X. Han, L. Gu, Z. Sun, M. Chen, Y. Zhang, L. Luo, M. Xu, S. Chen, H. Liu, J. Wan, Y. B. He, J. Chen, Q. Zhang, *Energy Environ. Sci.* **2023**, *16*, 5395.
[111] Y. An, H. Fei, G. Zeng, L. Ci, S. Xiong, J. Feng, T. Qian, *ACS Nano* **2018**, *12*, 4993.
[112] B. Lu, B. Ma, X. Deng, B. Wu, Z. Wu, J. Luo, X. Wang, G. Chen, *Chem. Eng. J.* **2018**, *351*, 269.
[113] Y. Son, S. Sim, H. Ma, M. Choi, Y. Son, N. Park, J. Cho, M. Park, *Adv. Mater.* **2018**, *30*, 1705430.
[114] J. Wu, Y. Cao, H. Zhao, J. Mao, Z. Guo, *Carbon Energy* **2019**, *1*, 57.
[115] W. Zeng, L. Wang, X. Peng, T. Liu, Y. Jiang, F. Qin, L. Hu, P. K. Chu, K. Huo, Y. Zhou, *Adv. Energy Mater.* **2018**, *8*, 1702314.
[116] S. Chen, Z. Song, L. Wang, H. Chen, S. Zhang, F. Pan, L. Yang, *Acc. Chem. Res.* **2022**, *55*, 2088.
[117] T. W. Kwon, Y. K. Jeong, E. Deniz, S. Y. Alqaradawi, J. W. Choi, A. Coskun, *ACS Nano* **2015**, *9*, 11317.
[118] Z. Xu, J. Yang, T. Zhang, Y. Nuli, J. Wang, S. Ichi Hirano, *Joule* **2018**, *2*, 950.
[119] C. Wang, H. Wu, Z. Chen, M. T. Mcdowell, Y. Cui, Z. Bao, *Nat. Chem.* **2013**, *5*, 1042.
[120] S. Choi, T. woo Kwon, A. Coskun, J. W. Choi, *Science* **2017**, *357*, 279.
[121] L. Hu, J. Wang, K. Wang, Z. Gu, Z. Xi, H. Li, F. Chen, Y. Wang, Z. Li, C. Ma, *Nat. Commun.* **2023**, *14*, 3807.
[122] L. Yang, Z. Wang, Y. Feng, R. Tan, Y. Zuo, R. Gao, Y. Zhao, L. Han, Z. Wang, F. Pan, *Adv. Energy Mater.* **2017**, *7*, 1701437.
[123] Y. Fu, K. Yang, S. Xue, W. Li, S. Chen, Y. Song, Z. Song, W. Zhao, Y. Zhao, F. Pan, L. Yang, X. Sun, *Adv. Funct. Mater.* **2023**, *33*, 2210845.
[124] B. Peng, Z. Liu, Q. Zhou, X. Xiong, S. Xia, X. Yuan, F. Wang, K. I. Ozoemena, L. Liu, L. Fu, Y. Wu, *Adv. Mater.* **2024**, *36*, 2307142.
[125] Q. Zhou, X. Yang, X. Xiong, Q. Zhang, B. Peng, Y. Chen, Z. Wang, L. Fu, Y. Wu, *Adv. Energy Mater.* **2022**, *12*, 2201991.
[126] T. Dai, S. Wu, Y. Lu, Y. Yang, Y. Liu, C. Chang, X. Rong, R. Xiao, J. Zhao, Y. Liu, W. Wang, L. Chen, Y. S. Hu, *Nat. Energy* **2023**, *8*, 1221.
[127] Z. Zhang, C. Feng, C. Liu, M. Zuo, L. Qin, X. Yan, Y. Xing, H. Li, R. Si, S. Zhou, J. Zeng, *Nat. Commun.* **2020**, *11*, 1215.
[128] J. Cheng, X. Yang, X. Yang, R. Xia, Y. Xu, W. Sun, J. Zhou, *Fuel Process. Technol.* **2022**, *229*, 107174.
[129] P. Bai, J. Li, F. R. Brushett, M. Z. Bazant, *Energy Environ. Sci.* **2016**, *9*, 3221.
[130] M. Yang, Y. Liu, Y. Mo, *Nat. Commun.* **2023**, *14*, 2986.
[131] J. Kasemchainan, S. Zekoll, D. Spencer Jolly, Z. Ning, G. O. Hartley, J. Marrow, P. G. Bruce, *Nat. Mater.* **2019**, *18*, 1105.
[132] Y. Liang, H. Liu, G. Wang, *Infomat* **2022**, *4*, e12292.
[133] X. Li, Z. Wang, H. Lin, Y. Liu, Y. Min, F. Pan, *Electrochim. Acta.* **2019**, *293*, 25.
[134] X. Xiong, Q. Qiao, Q. Zhou, X. Cheng, L. Liu, L. Fu, Y. Chen, B. Wang, X. Wu, Y. Wu, *Nano Res.* **2023**, *16*, 8448.
[135] X. Xiong, W. Yan, Y. Zhu, L. Liu, L. Fu, Y. Chen, N. Yu, Y. Wu, B. Wang, R. Xiao, *Adv. Energy Mater.* **2022**, *12*, 2103112.
[136] M. J. Wang, R. Choudhury, J. Sakamoto, *Joule* **2019**, *3*, 2165.
[137] H. Zheng, S. Wu, R. Tian, Z. Xu, H. Zhu, H. Duan, H. Liu, *Adv. Funct. Mater.* **2020**, *30*, 1906189.
[138] A. Sharafi, E. Kazyak, A. L. Davis, S. Yu, T. Thompson, D. J. Siegel, N. P. Dasgupta, J. Sakamoto, *Chem. Mater.* **2017**, *29*, 7961.
[139] J. F. Wu, B. W. Pu, D. Wang, S. Q. Shi, N. Zhao, X. Guo, X. Guo, *ACS Appl. Mater. Interfaces* **2019**, *11*, 898.
[140] L. Zhao, W. Li, C. Wu, Q. Ai, L. Guo, Z. Chen, J. Zheng, M. Anderson, H. Guo, J. Lou, Y. Liang, Z. Fan, J. Zhu, Y. Yao, *Adv. Energy Mater.* **2023**, *13*, 2300679.
[141] X. Xiong, R. Sun, W. Yan, Q. Qiao, Y. Zhu, L. Liu, L. Fu, N. Yu, Y. Wu, B. Wang, *J. Mater. Chem. A.* **2022**, *10*, 13814.
[142] T. Krauskopf, B. Mogwitz, C. Rosenbach, W. G. Zeier, J. Janek, *Adv. Energy Mater.* **2019**, *9*, 1902568.
[143] C. Wang, Y. Gong, B. Liu, K. Fu, Y. Yao, E. Hitz, Y. Li, J. Dai, S. Xu, W. Luo, E. D. Wachsman, L. Hu, *Nano Lett.* **2017**, *17*, 565.
[144] K. K. Fu, Y. Gong, Z. Fu, H. Xie, Y. Yao, B. Liu, M. Carter, E. Wachsman, L. Hu, *Angew. Chem. – Int. Ed.* **2017**, *56*, 14942.
[145] Y. Lu, X. Huang, Y. Ruan, Q. Wang, R. Kun, J. Yang, Z. Wen, *J. Mater. Chem. A.* **2018**, *6*, 18853.
[146] Y. Zhang, J. Meng, K. Chen, H. Wu, J. Hu, C. Li, *ACS Energy Lett.* **2020**, *5*, 1167.
[147] J. Fu, P. Yu, N. Zhang, G. Ren, S. Zheng, W. Huang, X. Long, H. Li, X. Liu, *Energy Environ. Sci.* **2019**, *12*, 1404.
[148] J. Duan, W. Wu, A. M. Nolan, T. Wang, J. Wen, C. Hu, Y. Mo, W. Luo, Y. Huang, *Adv. Mater.* **2019**, *31*, 1807243.
[149] C. Wang, Q. Sun, Y. Liu, Y. Zhao, X. Li, X. Lin, M. N. Banis, M. Li, W. Li, K. R. Adair, D. Wang, J. Liang, R. Li, L. Zhang, R. Yang, S. Lu, X. Sun, *Nano Energy* **2018**, *48*, 35.
[150] S. Jeong, V.-C. Ho, O. Kwon, Y. Park, J. Mun, *Energy Mater.* **2023**, *3*, 300048.
[151] M. Liu, L. Yang, H. Liu, A. Amine, Q. Zhao, Y. Song, J. Yang, K. Wang, F. Pan, *ACS Appl. Mater. Interfaces* **2019**, *11*, 32046.
[152] R. Gao, R. Tan, L. Han, Y. Zhao, Z. Wang, L. Yang, F. Pan, *J. Mater. Chem. A.* **2017**, *5*, 5273.
[153] K. Wang, L. Yang, Z. Wang, Y. Zhao, Z. Wang, L. Han, Y. Song, F. Pan, *Chem. Commun.* **2018**, *54*, 13060.
[154] Z. Wang, Z. Wang, L. Yang, H. Wang, Y. Song, L. Han, K. Yang, J. Hu, H. Chen, F. Pan, *Nano Energy* **2018**, *49*, 580.

[155] Z. Wang, J. Hu, L. Han, Z. Wang, H. Wang, Q. Zhao, J. Liu, F. Pan, *Nano Energy* **2019**, *56*, 92.
[156] J. Tao, L. Liu, J. Han, J. Peng, Y. Chen, Y. Yang, H. rong Yao, J. Li, Z. Huang, Y. Lin, *Energy Storage Mater.* **2023**, *60*, 102809.
[157] J. Y. Kim, S. Jung, S. H. Kang, J. Park, M. J. Lee, D. Jin, D. O. Shin, Y. G. Lee, Y. M. Lee, *Adv. Energy Mater.* **2022**, *12*, 2103108.
[158] W. D. Richards, L. J. Miara, Y. Wang, J. C. Kim, G. Ceder, *Chem. Mater.* **2016**, *28*, 266.
[159] Y. Zhu, X. He, Y. Mo, *J. Mater. Chem. A.* **2016**, *4*, 3253.
[160] C. Hänsel, S. Afyon, J. L. M. Rupp, *Nanoscale* **2016**, *8*, 18412.
[161] J. Auvergniot, A. Cassel, J. B. Ledeuil, V. Viallet, V. Seznec, R. Dedryvère, *Chem. Mater.* **2017**, *29*, 3883.
[162] X. Li, H. Guan, Z. Ma, M. Liang, D. Song, H. Zhang, X. Shi, C. Li, L. Jiao, L. Zhang, *J. Energy Chem.* **2020**, *48*, 195.
[163] W. Zhang, T. Leichtweiß, S. P. Culver, R. Koerver, D. Das, D. A. Weber, W. G. Zeier, J. Janek, *ACS Appl. Mater. Interfaces* **2017**, *9*, 35888.
[164] X. Li, Z. Ren, M. Norouzi Banis, S. Deng, Y. Zhao, Q. Sun, C. Wang, X. Yang, W. Li, J. Liang, X. Li, Y. Sun, K. Adair, R. Li, Y. Hu, T. K. Sham, H. Huang, L. Zhang, S. Lu, J. Luo, X. Sun, *ACS Energy Lett.* **2019**, *4*, 2480.
[165] Y.-L. Heng, Z.-Y. Gu, J.-Z. Guo, X.-T. Yang, X.-X. Zhao, X.-L. Wu, *Energy Mater.* **2022**, *2*, 200017.
[166] D. Cao, Y. Zhang, A. M. Nolan, X. Sun, C. Liu, J. Sheng, Y. Mo, Y. Wang, H. Zhu, *Nano Lett.* **2020**, *20*, 1483.
[167] C. Wang, X. Li, Y. Zhao, M. N. Banis, J. Liang, X. Li, Y. Sun, K. R. Adair, Q. Sun, Y. Liu, F. Zhao, S. Deng, X. Lin, R. Li, Y. Hu, T. Sham, H. Huang, L. Zhang, *Small Methods* **2019**, *3*, 1900261.
[168] A. Kim, F. Strauss, T. Bartsch, J. H. Teo, T. Hatsukade, A. Mazilkin, J. Janek, P. Hartmann, T. Brezesinski, *Chem. Mater.* **2019**, *31*, 9664.
[169] S. Deng, X. Li, Z. Ren, W. Li, J. Luo, J. Liang, J. Liang, M. N. Banis, M. Li, Y. Zhao, X. Li, C. Wang, Y. Sun, Q. Sun, R. Li, Y. Hu, H. Huang, L. Zhang, S. Lu, J. Luo, X. Sun, *Energy Storage Mater.* **2020**, *27*, 117.
[170] S. Yubuchi, Y. Ito, T. Matsuyama, A. Hayashi, M. Tatsumisago, *Solid State Ionics* **2016**, *285*, 79.
[171] S. Seki, Y. Kobayashi, H. Miyashiro, Y. Mita, T. Iwahori, *Chem. Mater.* **2005**, *17*, 2041.
[172] J. H. Woo, J. E. Trevey, A. S. Cavanagh, Y. S. Choi, S. C. Kim, S. M. George, K. H. Oh, S.-H. Lee, *J. Electrochem. Soc.* **2012**, *159*, A1120.
[173] N. Ohta, K. Takada, L. Zhang, R. Ma, M. Osada, T. Sasaki, *Adv. Mater.* **2006**, *18*, 2226.
[174] A. Y. Kim, F. Strauss, T. Bartsch, J. H. Teo, T. Hatsukade, A. Mazilkin, J. Janek, P. Hartmann, T. Brezesinski, *Chem. Mater.* **2019**, *31*, 9664.
[175] A. Sakuda, H. Kitaura, A. Hayashi, K. Tadanaga, M. Tatsumisago, *J. Electrochem. Soc.* **2009**, *156*, A27.
[176] F. Zhao, Y. Zhao, J. Wang, Q. Sun, K. Adair, S. Zhang, J. Luo, J. Li, W. Li, Y. Sun, X. Li, J. Liang, C. Wang, R. Li, H. Huang, L. Zhang, S. Zhao, S. Lu, X. Sun, *Energy Storage Mater.* **2020**, *33*, 139.
[177] S. H. Jung, K. Oh, Y. J. Nam, D. Y. Oh, P. Brüner, K. Kang, Y. S. Jung, *Chem. Mater.* **2018**, *30*, 8190.
[178] K. Takada, N. Ohta, L. Zhang, K. Fukuda, I. Sakaguchi, R. Ma, M. Osada, T. Sasaki, *Solid State Ionics* **2008**, *179*, 1333.
[179] H. Visbal, Y. Aihara, S. Ito, T. Watanabe, Y. Park, S. Doo, *J. Power Sources* **2016**, *314*, 85.
[180] S. K. Jung, H. Gwon, S. S. Lee, H. Kim, J. C. Lee, J. G. Chung, S. Y. Park, Y. Aihara, D. Im, *J. Mater. Chem. A* **2019**, *7*, 22967.
[181] J. Zheng, X. Zhu, L. Wang, J. Lu, T. Wu, *Mater. Chem. Front.* **2023**, *7*, 4810.
[182] D. Cao, T. Ji, A. Singh, S. Bak, Y. Du, X. Xiao, H. Xu, J. Zhu, H. Zhu, *Adv. Energy Mater.* **2023**, *13*, 2203969.
[183] S. Wenzel, T. Leichtweiss, D. Krüger, J. Sann, J. Janek, *Solid State Ionics* **2015**, *278*, 98.
[184] S. Bai, W. Bao, K. Qian, B. Han, W. Li, B. Sayahpour, B. Sreenarayanan, D. H. S. Tan, S. yeon Ham, Y. S. Meng, *Adv. Energy Mater.* **2023**, *13*, 2301041.
[185] D. H. S. Tan, E. A. Wu, H. Nguyen, Z. Chen, M. A. T. Marple, J. M. Doux, X. Wang, H. Yang, A. Banerjee, Y. S. Meng, *ACS Energy Lett.* **2019**, *4*, 2418.
[186] T. K. Schwietert, V. A. Arszelewska, C. Wang, C. Yu, A. Vasileiadis, N. J. J. de Klerk, J. Hageman, T. Hupfer, I. Kerkamm, Y. Xu, E. van der Maas, E. M. Kelder, S. Ganapathy, M. Wagemaker, *Nat. Mater.* **2020**, *19*, 428.
[187] D. H. S. Tan, Y. T. Chen, H. Yang, W. Bao, B. Sreenarayanan, J. M. Doux, W. Li, B. Lu, S. Y. Ham, B. Sayahpour, J. Scharf, E. A. Wu, G. Deysher, H. E. Han, H. J. Hah, H. Jeong, J. B. Lee, Z. Chen, Y. S. Meng, *Science* **2021**, *373*, 1494.
[188] H. Liu, Q. Sun, H. Zhang, J. Cheng, Y. Li, Z. Zeng, S. Zhang, X. Xu, F. Ji, D. Li, J. Lu, L. Ci, *Energy Storage Mater.* **2023**, *55*, 244.
[189] Y. Huang, B. Shao, Y. Wang, F. Han, *Energy Environ. Sci.* **2023**, *16*, 1569.
[190] X. Zhan, M. Li, S. Li, X. Pang, F. Mao, H. Wang, Z. Sun, X. Han, B. Jiang, Y. B. He, M. Li, Q. Zhang, L. Zhang, *Energy Storage Mater.* **2023**, *61*, 102875.
[191] W. Yan, Z. Mu, Z. Wang, Y. Huang, D. Wu, P. Lu, J. Lu, J. Xu, Y. Wu, T. Ma, M. Yang, X. Zhu, Y. Xia, S. Shi, L. Chen, H. Li, F. Wu, *Nat. Energy* **2023**, *8*, 800.
[192] Y. Zhu, X. He, Y. Mo, *ACS Appl. Mater. Interfaces* **2015**, *7*, 23685.
[193] A. Schwöbel, R. Hausbrand, W. Jaegermann, *Solid State Ionics* **2015**, *273*, 51.
[194] L. Yang, Y. Song, H. Liu, Z. Wang, K. Yang, Q. Zhao, Y. Cui, J. Wen, W. Luo, F. Pan, *Small Methods* **2020**, *4*, 19000751.
[195] S. Yuan, M. J. Zhang, X. Yang, Z. Mei, Y. Chen, F. Pan, *RSC Adv.* **2017**, *7*, 23415.
[196] B. Wu, S. Wang, J. Lochala, D. Desrochers, B. Liu, W. Zhang, J. Yang, J. Xiao, *Energy Environ. Sci.* **2018**, *11*, 1803.
[197] H. Duan, W. P. Chen, M. Fan, W. P. Wang, L. Yu, S. J. Tan, X. Chen, Q. Zhang, S. Xin, L. J. Wan, Y. G. Guo, *Angew. Chem. – Int. Ed.* **2020**, *59*, 12069.
[198] R. Xu, F. Han, X. Ji, X. Fan, J. Tu, C. Wang, *Nano Energy* **2018**, *53*, 958.
[199] Y. Liu, Q. Sun, Y. Zhao, B. Wang, P. Kaghazchi, K. R. Adair, R. Li, C. Zhang, J. Liu, L. Kuo, Y. Hu, T. Sham, L. Zhang, R. Yang, S. Lu, X. Song, X. Sun, *ACS Appl. Mater. Interfaces* **2018**, *10*, 31240.
[200] Y. Liu, C. Li, B. Li, H. Song, Z. Cheng, M. Chen, P. He, *Adv. Energy Mater.* **2018**, *8*, 1702374.
[201] Q. Cheng, A. Li, N. Li, Q. Cheng, A. Li, N. Li, S. Li, A. Zangiabadi, T. Li, W. Huang, *Joule* **2019**, *3*, 1510.
[202] X. Hao, Q. Zhao, S. Su, S. Zhang, J. Ma, L. Shen, Q. Yu, *Adv. Energy Mater.* **2019**, *6*, 1901604.
[203] F. Javier, Q. Cortes, M. T. Mcdowell, J. A. Lewis, J. Tippens, T. S. Marchese, *J. Electrochem. Soc.* **2020**, *167*, 050502.
[204] Q. Yu, D. Han, Q. Lu, Y. He, S. Li, Q. Liu, C. Han, F. Kang, B. Li, *ACS Appl. Mater. Interfaces* **2019**, *11*, 9911.
[205] L. He, Q. Sun, C. Chen, J. An, S. Oh, J. Sun, M. Li, W. Tu, H. Zhou, K. Zeng, L. Lu, *ACS Appl. Mater. Interfaces* **2019**, *4*, 20895.
[206] W. Zhou, S. Wang, Y. Li, S. Xin, A. Manthiram, J. B. Goodenough, *J. Am. Chem. Soc.* **2016**, *138*, 9385.
[207] H. Huo, J. Liang, N. Zhao, X. Li, X. Lin, Y. Zhao, K. Adair, R. Li, X. Guo, X. Sun, *ACS Energy Lett.* **2020**, *5*, 2156.
[208] J. Morey, J. B. Ledeuil, H. Martinez, L. Madec, *J. Mater. Chem. A* **2023**, *11*, 9512.
[209] Z. Liang, Y. Xiang, K. Wang, J. Zhu, Y. Jin, H. Wang, B. Zheng, Z. Chen, M. Tao, X. Liu, Y. Wu, R. Fu, C. Wang, M. Winter, Y. Yang, *Nat. Commun.* **2023**, *14*, 259.

[210] Y. Chen, Z. Wang, X. Li, X. Yao, C. Wang, Y. Li, W. Xue, D. Yu, S. Y. Kim, F. Yang, A. Kushima, G. Zhang, H. Huang, N. Wu, Y. W. Mai, J. B. Goodenough, J. Li, *Nature* **2020**, *578*, 251.
[211] B. Zhang, R. Tan, L. Yang, J. Zheng, K. Zhang, S. Mo, Z. Lin, F. Pan, *Energy Storage Mater.* **2018**, *10*, 139.
[212] B. Zhang, Z. Lin, L. W. Wang, F. Pan, *ACS Appl. Mater. Interfaces* **2020**, *12*, 6007.
[213] B. Zhang, Z. He, J. Zhong, L. Yang, Z. Lin, F. Pan, *J. Mater. Chem. A.* **2021**, *9*, 22952.
[214] B. Zhang, M. Weng, Z. Lin, Y. Feng, L. Yang, L. W. Wang, F. Pan, *Small* **2020**, *16*, 1906374.
[215] B. Zhang, J. Zhong, Y. Zhang, L. Yang, J. Yang, S. Li, L. W. Wang, F. Pan, Z. Lin, *Nano Energy* **2021**, *79*, 105440.

Zhikang Deng obtained his bachelor's degree from School of Metallurgy and Environment at Central South University (China) in 2022. He is currently studying for the master's degree under the guidance of Prof. Feng Pan in the School of Advanced Materials, Peking University. His research interests include advanced solid electrolytes and interphases in lithium-ion batteries.

Shiming Chen received his bachelor's degree from the Institute for Advanced Study, Nanchang University (China) in 2020. He is currently a PhD candidate under the supervision of Prof. Feng Pan in School of Advanced Materials, Peking University Shenzhen Graduate School, China. His research focuses on the anode materials of lithium-ion batteries and quantum chemical calculation.

Kai Yang is a Lecturer in the Advanced Technology Institute at the University of Surrey. He received his PhD degree from the School of Advanced Materials at Peking University Shenzhen Graduate School in Prof. Feng Pan's group. His research interests mainly focus on developing in situ characterizations for interfacial research in energy storage/conversion material and devices, developing composite solid electrolytes for SSBs, carbon dioxide fixation and utilization technologies such as Li/Na/Zn-CO_2 battery, and developing nanoelectronics platforms for energy applications.

Yongli Song received his bachelor degree from the Department of Physics at Harbin Institute of Technology (HIT, China) in 2010 and earned PhD degree from HIT in 2017, He is currently an equivalent professor at Jiangsu University (China). His research interests mainly focus on solid-state batteries and solid-state electrolytes.

Shida Xue received his bachelor's degree from the Department of Chemistry at South China Normal University (China) in 2019 and earned PhD degree from the School of Advanced Materials at Peking University Shenzhen Graduate School in Prof. Feng Pan's group. His research focuses on the interfacial mechanisms and modification of composite solid-state electrolytes.

Xiangming Yao obtained his bachelor's degree from the College of Materials Science and Engineering at Donghua University (China) in 2021. He earned his master's degree under the guidance of Prof. Feng Pan at the School of Advanced Materials, Peking University Shenzhen Graduate School. His research interests include inorganic solid electrolytes and composite solid-state electrolytes.

Luyi Yang received his bachelor's degree from the Department of Chemistry at Xiamen University (China) in 2010 and earned PhD degree from the School of Chemistry at Southampton University (U.K.) in 2015. He is currently an associate research professor at the School of Advanced Materials, Peking University, Shenzhen Graduate School. His research interests mainly focus on the investigation of interphases in lithium-ion batteries through advanced characterization techniques.

Feng Pan, chair professor of Peking University, Vice President of Shenzhen Graduate School of Peking University, Founding Dean of the School of New Materials, Member of the Chinese Chemical Society, Executive editor of Structural Chemistry. He has long been committed to the development of structural chemistry methodology and its application in the research and development of new materials, created the structural chemistry theory based on graph theory, established the in situ dynamic structure characterization system based on large scientific devices such as neutron and synchrotron radiation, and explored and revealed the material genes and structure-function relationship. Breakthroughs have been made in solving scientific problems such as lithium battery energy storage density, power density and stability. He has published more than 430 SCI articles in well-known journals such as Nature (2), Nature Energy (1) and Nature Nanotechnology (3) as the corresponding author. He has been awarded with the China Electrochemical Contribution Award and the Battery Technology Award of the American Electrochemical Society.